European Journal of Medicinal Chemistry 207 (2020) 112813

Contents lists available at ScienceDirect

European Journal of Medicinal Chemistry

journal homepage: http://www.elsevier.com/locate/ejmech

Research paper

Design, synthesis and comparative analysis of triphenyl-1,2,3-triazoles as anti-proliferative agents

Divya Dheer [a, e, 1], Chittaranjan Behera [b, 1], Davinder Singh [a, e], Mohd Abdullaha [c, e], Gousia Chashoo [d], Sandip B. Bharate [c, e], Prem N. Gupta [b, e, **], Ravi Shankar [a, e, *]

[a] Bio-organic Chemistry Division, CSIR-Indian Institute of Integrative Medicine, Jammu, 180001, India
[b] PK-PD Toxicology & Formulation Division, CSIR-Indian Institute of Integrative Medicine, Jammu, 180001, India
[c] Medicinal Chemistry Division, CSIR-Indian Institute of Integrative Medicine, Jammu, 180001, India
[d] Cancer Pharmacology Division, CSIR-Indian Institute of Integrative Medicine, Jammu, 180001, India
[e] Academy of Scientific and Innovative Research (AcSIR), New Delhi, 110025, India

ARTICLE INFO

Article history:
Received 22 July 2020
Received in revised form
18 August 2020
Accepted 2 September 2020
Available online 9 September 2020

Keywords:
Breast cancer
1,2,3-Triazole
Estrogen receptor
Molecular docking studies
Apoptosis
Morphological alteration

ABSTRACT

Herein, a series of triaryl-1,2,3-triazoles, in order to check cytotoxicity on breast cancer cell lines have been synthesized with pendent benzyl ring to mimic the phenolic **A** ring of Tamoxifene. The biological results indicated that most of the compounds possessed comparative anti-proliferative activities in both ER + *ve* (MCF-7) and ER−*ve* (MDA-MB-231) breast cancer cell lines. Among synthesized derivatives, five compounds **8f**, **8i**, **8j**, **8n** and **8p** showed anti-proliferative activities at <5 μM against MCF-7 cell line and three compounds **8e**, **8f** and **8j** show IC_{50} value greater than 30 μM in FR-2 cells (normal cell). Moreover, to understand the mechanistic behavior of the selective compound **8f,** various studies performed viz. surface morphological changes by bright field microscopic examination, nuclear morphological alteration by DAPI staining, measurement of intracellular ROS level and determination of change in mitochondrial membrane potential. It was observed that, the selective compound **8f** associated with higher ROS generation along with decrease in mitochondrial membrane potential in addition to surface and nuclear morphological alterations such as reduction in number and shrinkage of cells coupled with nuclear blabbing indicating sign of apoptosis. Further, molecular docking study in comparison to tamoxifen was also carried out to investigate the interaction of **8f** with ER-α which favors its possible mode of anticancer action.

1. Introduction

Nitrogen-based heterocycles are structural motifs of biological interest in various disciplines, namely, anticancer, antinociceptive, antipyretic, antimicrobial, antiepileptic, antituberculotic, antiviral, anticoagulant as well antiplatelet agents and several synthesized compounds have been approved by the FDA [1,2]. Towards this direction, triazoles have turned out to be the most effective moieties against different tumor cells [3–5]. Some of the hybrid compounds containing 1,2,3-1*H*-triazole tethered with various natural products have shown promising in vitro anticancer results [6–9]. Some of the triazoles, namely, anastrozole (Arimidex) (**1**) and letrozole (Femara) (**2**) are clinically available third-generation aromatase inhibitors that exhibits opposed effects on the ER (estrogen receptor) expression of breast cancer cells, showing superior therapeutic effects over antiestrogens. These triazoles inhibit the aromatase enzyme by binding of the N-4 nitrogen of the triazole ring with the heme iron atom of the CYP19 enzyme complex also proving contraindication in premenopausal women including pregnant and lactating women [10]. Therefore, there comes a need for novel compounds which can overcome such limitations.

ERβ has also shown clinical advancement in the prevention of colorectal carcinoma [11,12]. Non-steroidal drugs which interact with ER have already proven useful in contraceptives, uterine dysfunction, osteoporosis as well as for the treatment of breast cancer [13]. Some of the other examples of triphenylethylene based

* Corresponding author. Bio-organic Chemistry Division, CSIR-Indian Institute of Integrative Medicine, Jammu, 180001, India.
** Corresponding author. PK-PD Toxicology & Formulation Division, CSIR-Indian Institute of Integrative Medicine, Jammu, 180001, India.
E-mail addresses: pngupta@iiim.res.in (P.N. Gupta), rshankar@iiim.res.in (R. Shankar).
[1] Both authors contributed equally.

https://doi.org/10.1016/j.ejmech.2020.112813
0223-5234/

SERMs include raloxifene (**3**), nafoxidine (**4**) and lasofoxifene (**5**). On the other hand, Tamoxifen (**6**) has been the drug of choice for last 30 years for estrogen related positive breast tumors. Tamoxifen being cheaper compared to other anti-estrogen drugs can very well increase the cure rate by 10% especially in case of low- and middle-income countries but the selectively of combined actions of agonists and antagonists has been minimal. Novel molecules having increased selectively signify the most active biological potential accompanied by least adverse outcomes. In fact, some of the estrogen receptor dependent α- (**7**) or β- (**8**) agonists are already in clinical trials and Katzenellenbogen group have also innovated the concept of antiestrogens with a wide variety of pyrazole based molecules as depicted in Fig. 1.

Numerous literature reports have shown triphenylethylene as well as benzothiopene derivatives to be successful ER molecules and the triaryl substituted pyrazole-related ER antagonists exhibiting remarkable therapeutic potential is also widely recognized [14]. For instance, Katzenellenbogen and group in 1999 explored a novel series of triaryl-substituted pyrazole based ligand molecules showing high affinity for ER [15]. According to the study, propylpyrazoletriol (PPT) (**7**) was observed to be the best compound of the series which binded well with 410-fold affinity for ER-α receptor [16]. Continuing their research, they discovered that the above pyrazole ER agonist molecule, if converted into its antagonist by embracing them with a basic side chain, might act in the similar manner, as in case of raloxifene. Based on the above study, C (5) piperidinyl-ethoxy substituted pyrazole exhibited 20-fold higher affinity towards ER-α better than ER-β subtype [17]. Later, Hajela group in 2008 investigated new tetrazolyl indole derivatives containing *N*-ethyl amino moiety and observed 100% contraceptive efficacy at animal dose 10 mg/kg [18]. The same group synthesized 3,4,6-triaryl-2-pyranones [19] as well as hydrazone [20] derivatives as a new class of anti-breast tumor compounds. Recently, Katzenellenbogen group has again derivatized a large library of triaryl pyrazoles which hold a great promise as anti-inflammatory drugs [21]. Based on these observations, we have designed 1,2,3-triazoles as the cyclic prototype of triaryl substituted pyrazoles corresponding to triphenylethylene derivatives in adherence to specified positioning having three phenyl substitutions for therapeutic benefits.

The rationale behind the designing of 1,2,3-triazole based compounds was to construct a scaffold having specified arrangement bearing three phenyl substitutions in accordance to the reported leads such as propylpyrazoletriol (PPT) (**7**), tamoxifene and estradiol that are suitable to bind with its receptor. The 1,2,3-triazole ring represents the central core of the whole compound and three phenyl rings existed perfectly arranged to prove the ideal geometry of molecules further imitating PPT framework. Compared to PPT, the main differences in our present work are (i) the presence of extra nitrogen in the core that can enhance an interaction of molecule with receptors; (ii) the existence of bendable benzyl group (**ring 1**) that may help in adaptation of a favorable conformation change within the receptor cavity (Fig. 2) [22]. Furthermore, basic amino chains at *para* position of **ring 2** ease the association of ER proteins to give desired effect.

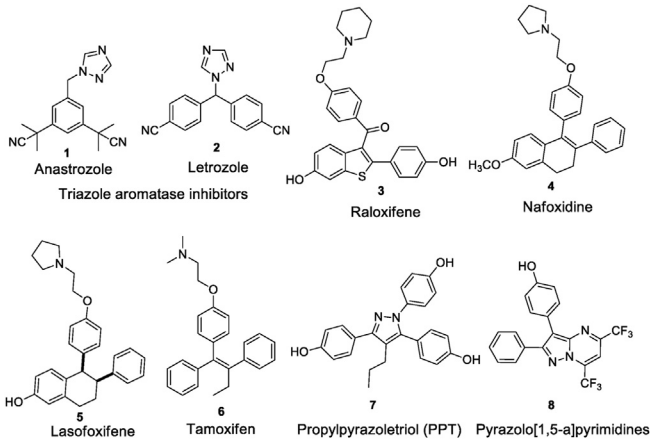

Fig. 1. Chemical structures of non-steroidal antiestrogens and triazole based aromatase inhibitors.

2. Results and discussion

2.1. Chemistry

Initially, 5-iodo-1,4-disubstituted-1,2,3-triazoles (**3a-3d**) were synthesized through copper (I)- catalyzed version of azide-alkyne cycloaddition reaction, using phenylacetylene, I_2 in DMF and benzyl bromide, sodium azide in triethylamine, along with the emergence of in situ 1-iodophenylacetylene and aryl azide (Scheme 1) [22]. In our previous work, we were able to synthesize **3a-3d** as well as **4a-4d** in-situ from benzyl bromide **1** and phenylacetylene **2** in the ratio of 80:20 approximately. Infact, I_2 as well as phenylacetylene **2** were shaken in aqueous medium in addition to CuI/β-CD (β-cyclodextrin) for half an hour. The emergence of 1-iodophenyacetylene was confirmed through its isolation and characterization by proton NMR. Thenceforth, benzyl bromide **1** plus NaN_3 were stirred in the same flask in the presence of elevated heat conditions close to 90 ^{O}C. Surprisingly, 1-Benzyl-5-iodo-4-phenyl-1*H*-1,2,3-triazole **3a** was yielded as major compound (79%). On the other hand, 1-Benzyl-4-phenyl-1*H*-1,2,3-triazole **4a** was obtained as minor compound when all the reactants were added synchronously. Based on NMR characterization, presence of iodine in triazole derivatives **3a-3d** was confirmed through a sharp singlet at δ76 in carbon spectrum. Whereas, in 5*H*-triazole compounds **4a-4d**, proton NMR showed the presence of a resonance peak at δ 7.6 as singlet but absence of δ 76 in carbon spectrum.

In the next step, Suzuki reaction was carried out in the presence of 4-hydroxyphenylboronic acids to form (**6a-6d**) (Scheme 2) [23]. Simultaneously, without iodo-triazole compound **4** obtained as byproduct in the same reaction mixture, has been further utilized to get **6a** via tosylation after having 4-(1-benzyl-4-phenyl-1H-1,2,3-triazol-5-yl)phenyl 4-methylbenzenesulfonate **5** as an intermediate (Scheme 2) [24,25].

Further in the method, alkyl chains were propagated with the help of various alkylating reagents to obtain 1-benzyl-5-(4-(2-

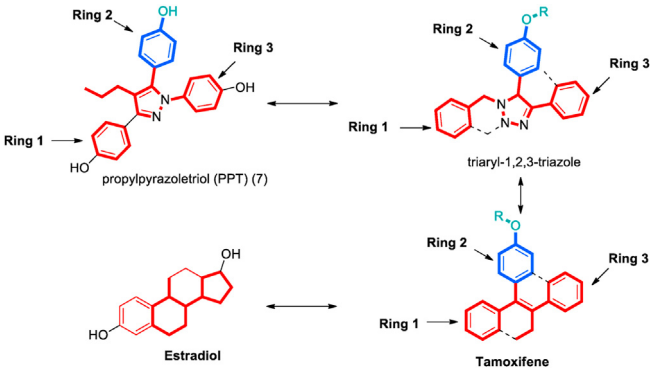

Fig. 2. Structural resemblance of 1,2,3-triazole based molecule to tamoxifen, estradiol and propylpyrazoletriol (PPT).

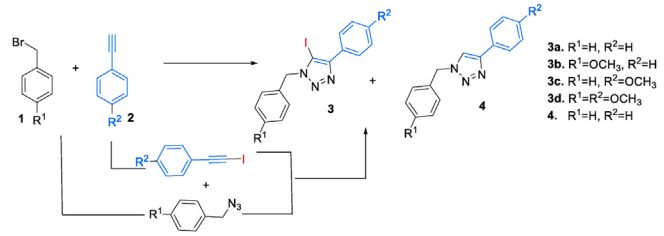

Scheme 1. Synthesis of iodo and without iodo-triazoles. **Reaction and conditions**: **1** (1.0 mmol), **2** (1.0 mmol), NaN_3 (2.0 mmol), I_2 (1.5 mmol), β-CD (1.0 mol %) CuI (10 mol %), Water (5 mL), open flask, 90 °C, 2–4 h.

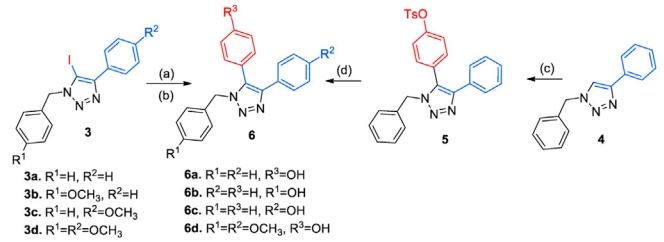

Scheme 2. Synthesis of triaryl-substituted 1,2,3-triazoles. **Reaction and Conditions:** (a) **3** (1.38 mmol), $PhB(OH)_2$ (2.07 mmol), K_2CO_3 (3.45 mmol), $PdCl_2(PPh_3)_2$ (10 mol%), DMF:H_2O (2.5:0.5) 6 mL; (b) **3b or 3c** (1 mmol), 1 M BCl_3 in DCM (5 mmol), −60 °C, 2–4 h; (c) **4** (1.27 mmol), 4-bromophenyl 4-methylbenzenesulfonate (0.85 mmol), $Pd(OAc)_2$ (4.0 mol%), PCy_3 (8.0 mol%), K_2CO_3 (2 equiv., 1.69 mmol), toluene (2 mL), N_2 atm., 22 h, 120 °C; (d) **5** (1 mmol), aq. NaOH solution (1 M), acetone (10 mL), reflux, 4–5 h.

chloroethoxy)phenyl)-4-phenyl-1*H*-1,2,3-triazole **7a** (**7a-7f**). Next step included the amination of above compounds, with different amines like pyrrolidine, piperidine, diethylamine or morpholine to form final active compounds (**8a-8p**). Desired methodology has been depicted below (Scheme 3).

Hydroxy functional group plays a very important role to enhance biological activity therefore; we have tried demethylation of active synthesized dimethoxy compounds **6d** to check the effect of methoxy group in biological activity. Compound **6d** was treated with BBr_3 in DCM at −78 °C to get demethylated compound but unfortunately, we obtained N-debenzylated compound

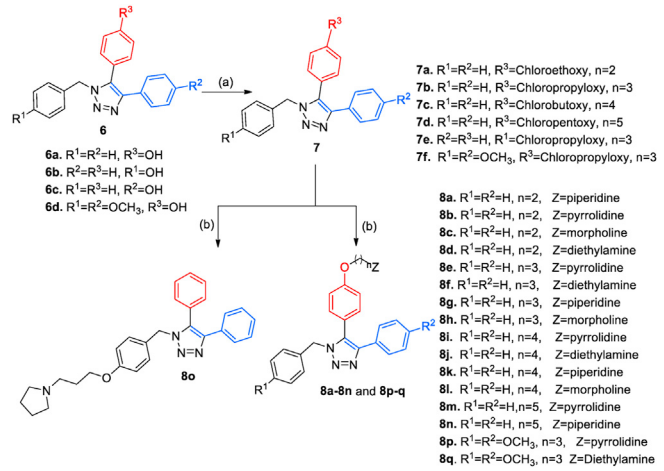

Scheme 3. Synthesis of aminated triaryl-substituted 1,2,3-triazoles. **Reaction and Conditions:** (a) **6** (0.15 mmol), halo alkanes (0.30 mmol), K_2CO_3 (0.30 mmol), acetone (10 mL), reflux, 4–5 h; (b) **7** (1.12 mM), amine (2 equiv), TBAI (10 mg), dry DMF (15 mL), 70–75 °C, 7 h.

(**6e**), which was confirmed by proton NMR with the absence of another set of 4 protons. No phenyl-H compound was found which was further confirmed by mass $[M+H]^+$ 268.1078 (Scheme 4).

2.2. Biological activity

2.2.1. Antitumoral activity against breast & colon tumor cells

The designed derivatives (**6a-6e**) and (**8a-8p**) were investigated for antitumoral activity and results indicated that most of the compounds possessed comparative anti-proliferative activities in MCF-7, MDA-MB-231 and HCT-116 cancer cells using SRB assay. Most synthesized compounds inhibited the growth of cancer cells at IC_{50} of less than 50 μM. Among synthesized derivatives, six compounds **8f** (3.5 μM), **8i** (4. 7 μM), **8j** (3.5 μM), **8n** (3.9 μM), **8p** (4.5 μM) and **8q** (3.3 μM) showed anti-proliferative activities at less than 5 μM against MCF-7 cell line and three compounds **8e** (30.8 μM), **8f** (34.8 μM) and **8j** (29.0 μM) showed IC_{50} value > 30 μM in FR-2 cells. Five of these, **8e**, **8f**, **8g**, **8i** and **8j** inhibited the growth of both MCF-7 as well as MDA-MB-231 cell lines at IC_{50} below 20 μM (Table 1). Three of these, **8b**, **8m** and **8n** were active against MCF-7 cell line selectively. Dimethoxy derivative of compound **8q** was also synthesized and evaluated against MCF-7 cell line but no improvement was observed therefore, its activity against another cell line was not evaluated. N-debenzylated compound **8q** also showed decrease in activity which confirmed the importance of N-benzyl group in biological action. Activity of compound **8f** was evaluated towards MCF-7, MDA-MB-231 as well as HCT-116 tumor cells at different concentrations of 0.1, 1, 10, 50 and 100 μM. Selective destruction of tumor cells while guarding development of healthy cells plays a pivotal characteristic among cytoprotectives. Nine active derivatives were investigated against FR-2 (normal breast epithelial) cell line at density of 10,000 cell/well for possible cytotoxicity. As shown in Table 1, the IC_{50} values of compounds **8e**, **8f** and **8j** were found to be greater than 30 μM in FR-2 cell line which further showed remarkably higher activity as compared to MCF-7 (5.7, 3.5 and 3.5 μM), and MDA-MB-231 (15.28, 15.54 and 9.61 μM respectively), demonstrating that these molecules **8e**, **8f** and **8j** having reduced toxicity towards healthy human cells compared to tumor cells.

The selected test compounds were screened against normal breast epithelial cell line FR-2 and cytotoxic selectivity of these compounds was evaluated by calculating the selectivity index based on the below mentioned formula:

$$SI = IC_{50}^{\text{non-cancerous cells}}/IC_{50}^{\text{cancer cells}}$$

Infact, SI greater than and equals to 10 has been marked as selective molecule [26]. In Table 1, selectivity index of nine compounds has been mentioned, out of which only compound **8f** having SI ≥ 10 was considered to be a selective one and therefore used for further investigation. The selectivity index of active compounds has also been discussed in Table 1. In fact, the increase in the percent growth inhibition has been observed with the increase in dose of compound **8f** (Fig. 3).

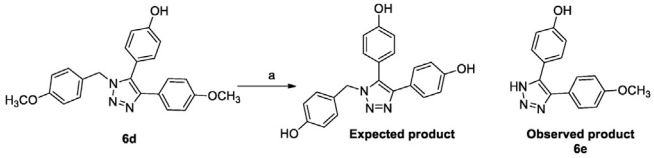

Scheme 4. Reaction and Conditions: (a) BCl_3, DCM, −70 °C, rt, 6 h

Table 1
Cytotoxic activities of target molecules against breast and colon cancer, normal cell lines along with their selectivity index.

Compd No	IC_{50} (Mean ± SD, μM)				
	MCF-7	MDA-MB-231	HCT-116	FR-2	Selectivity Index (SI)
6a	53.2 ± 0.87	23.36 ± 1.71	42.51 ± 2.06		
6b	77.5 ± 2.76	>100	>100		
6c	68.6 ± 1.74	94.42 ± 2.72	74.18 ± 4.1		
6d	22.6 ± 0.66	34.88 ± 2.06	38.31 ± 1.07		
6e	>100	95.87 ± 3.25	71.52 ± 0.83		
8a	45.97 ± 2	83.05 ± 2.8	51.68 ± 1.81		
8b	**7.1 ± 0.25**	**40.3 ± 0.79**	**25.53 ± 1.77**	14.5 ± 1.49	2.04
8c	27.21 ± 0.85	52.67 ± 0.39	33.23 ± 2.61		
8d	33.3 ± 1.2	52.86 ± 1.02	20.73 ± 2.11		
8e	**5.7 ± 0.3**	**15.28 ± 0.35**	**71.19 ± 2.08**	**30.8 ± 0.88**	5.4
8f	**3.5 ± 2.26**	**15.54 ± 0.6**	**30.43 ± 3.1**	**34.8 ± 1.17**	9.94
8g	**8.5 ± 0.4**	**19.43 ± 0.24**	**21.17 ± 2.8**	20.66 ± 1.18	2.43
8h	12.8 ± 3.89	29.1 ± 0.36	23.37 ± 2.2		
8i	**4.7 ± 0.25**	**10.32 ± 0.49**	**36.5 ± 2.36**	17.63 ± 1.4	3.75
8j	**3.5 ± 0.2**	**9.61 ± 0.67**	**13.74 ± 2.06**	**29.07 ± 2.33**	8.3
8k	46.17 ± 2.03	40.86 ± 1.48	39.66 ± 2.7		
8l	57 ± 1.34	99.76 ± 1.08	27.03 ± 2.54		
8m	**8.8 ± 1.36**	**46.51 ± 1.56**	**29.60 ± 2.83**	12.08 ± 1.27	1.37
8n	**3.95 ± 0.15**	**28.64 ± 2.05**	**83.11 ± 3.3**	10.13 ± 1.3	2.5
8o	34.4 ± 1.2	30.2 ± 1.17	28.37 ± 3.6		
8p	**4.56 ± 0.12**	**16.92 ± 1.18**	**19.39 ± 2.4**	17.53 ± 2.1	3.9
8q	3.33 ± 0.11	ND	ND		
Tamoxifen citrate	**9.53 ± 1.3**	**10.71 ± 1.55**	ND	22.3 ± 2.8	2.33

Note: ND = not determined.

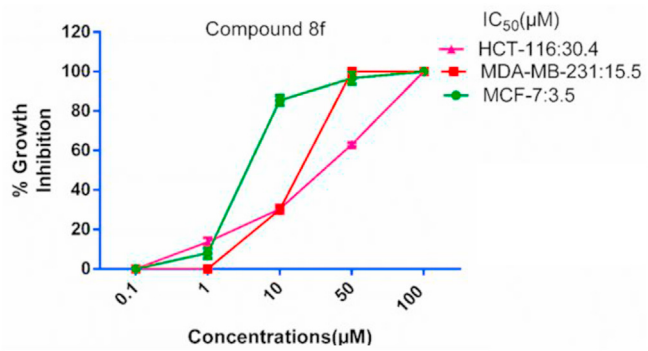

Fig. 3. Graphical representation of growth inhibition on different concentrations of compound **8f** againts **MCF-7**,**MDZ-MB-231** as well as **HCT-116** tornor cells assessed through **SRB** assay.

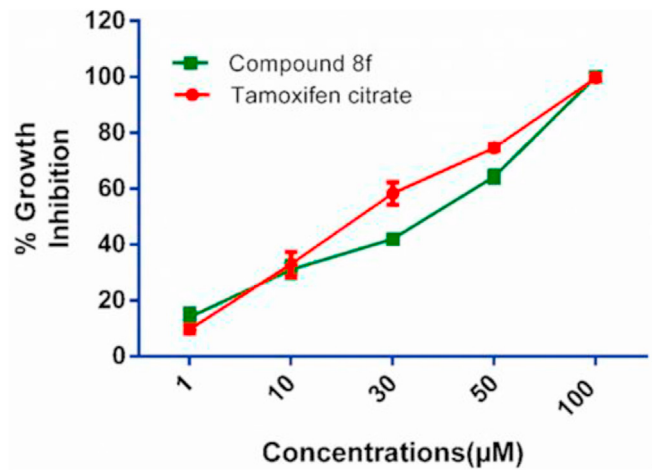

Fig. 4. Comparison of cell inhibition of compound **8f** and Tarnoxifen citrate against FR-2 cell line.

Compound **8f** was found selective against normal breast epithelial FR-2 cells with a selectivity index of 9.94 for **8f** and 2.33 for tamoxifen hence, exhibiting better cytotoxicity against MCF-7 cells (Fig. 4).

2.2.2. Assessment of cellular death caused due to compound 8f using bright field microscopy

Using bright field microscopy, the surface morphological changes were assessed by treating with compound **8f** in MCF-7 cells (Fig. 5). Random fields under bright light were examined following to the treatment with **8f** compound at various concentrations against MCF-7 cells for 48 h using inverted microscope. On viewing the wells of the six well tissue culture plate, visible rounding, shrinking of cell size and finally reduced cell number with disturbed morphology in comparison to the untreated control cells were visible among treated batches justifying inhibition of cell with compound **8f**. In addition to these, the positive control groups also show cellular death at 9.5 μM dose which was quiet high in comparison to the compound **8f** dose against MCF-7 cell line.

2.2.3. Compound 8f altered nuclear morphology assessed by DAPI staining

In the present study, DAPI staining helped to distinguish between the normal and apoptotic cells by the nuclear morphological changes caused after the treatment with **8f** compound against MCF-7 cell line in a concentration dependent manner. The morphological changes occurred can be visualized using fluorescence microscopy (Fig. 6). The nuclei of untreated cells appeared like more or less rounded structures while the treatment groups (**8f**) including tamoxifen showed chromatin condensation, nuclear blabbing and formation of apoptotic bodies. The nuclear morphological changes except the untreated control clearly suggested that MCF-7 cells had undergone

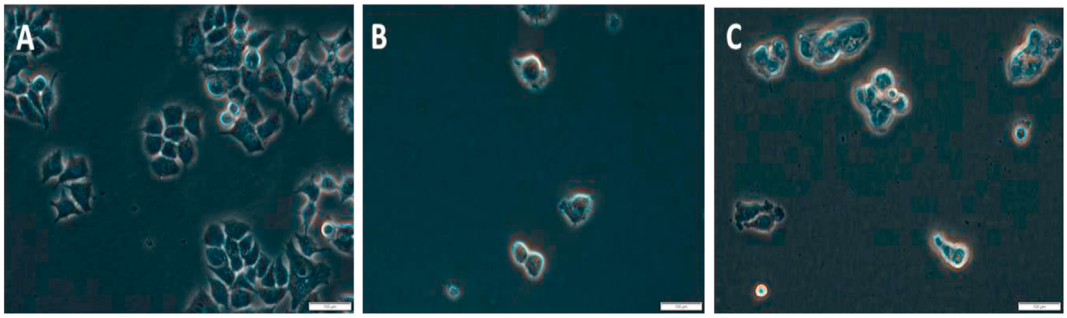

Fig. 5. Bright field microscopic examination of untreated and treated cells revealed surface morphology. (**A**) The untreated cells possess microvilli on cell surface and typical patchy formed structures. (**B**) Treated with standard drug tamoxifen at 9.5 μM showed apoptotic behavior in MCF-7 cells (**C**) After treatment with compound **8f** with 3.5 μM concentration for 48 h causes shrinkage, loss of microvilli, and apoptosis.

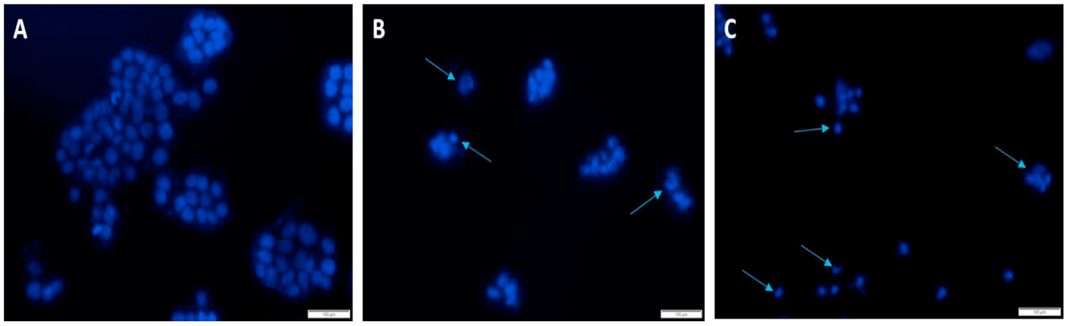

Fig. 6. DAPI staining assay of MCF-7 cells. The cells upon treatment with compound **8f** for 48 h stained with DAPI and examined for morphological changes. (**A**) Untreated cells represent normal rounded nuclear morphology whereas (**B**) tamoxifen 9.5 μM showed typical apoptotic bodies formed (**C**) MCF-7 cells treated with 3.5 μM of compound 8f showed nuclear morphological changes with visibly reduction in cell number and condensed chromatin structure. Arrows depicts the formation of apoptotic bodies.

apoptosis. This is the first report for the induction of apoptosis caused due to the anticancer compound **8f.**

2.2.4. Treatment of 8f molecule to enhanced intracellular ROS production in MCF-7 cells

Higher level of reactive oxygen species generation is a prime indication of apoptosis in cancer cells. In the current study, MCF-7 cells were incubated with DCFDA dye and intracellular ROS observed using a fluorescence microscope. Higher amount of ROS was produced in the positive control group. In a similar way, the amount of ROS was increased after the treatment with compound **8f** at 3.5 μM concentration. Observation through fluorescence microscope is a qualitative means of ROS generation in MCF-7 breast cancer cells where a sharp increase in fluorescence intensity was observed (Fig. 7). This study indicated that compound **8f** triggered ROS generation in MCF-7 cells which are a key feature of apoptosis.

2.2.5. Compound 8f induces depletion of mitochondrial membrane potential (MMP) in MCF-7 cell lines

Reduction of MMP ($\Delta\Psi m$) is the main characteristic of apoptosis. To assess the effect of **8f** molecule, loss of MMP was observed through fluorescence microscopy using rhodamine-123 staining (Fig. 8). After 48 h treatment with compound **8f** against MCF-7 cells, it was observed that the significant reduction in MMP in 3.5 μM concentration treatment group was due to the decrease in their fluorescence intensities which clearly justified the mitochondrial membrane destabilization in comparison to untreated cells. The result was quiet similar in case of tamoxifen treatment group. The MMP loss for compound **8f** has also not been reported in earlier studies and the data indicated that apoptosis was induced by treatment with **8f** molecule due to the loss of MMP.

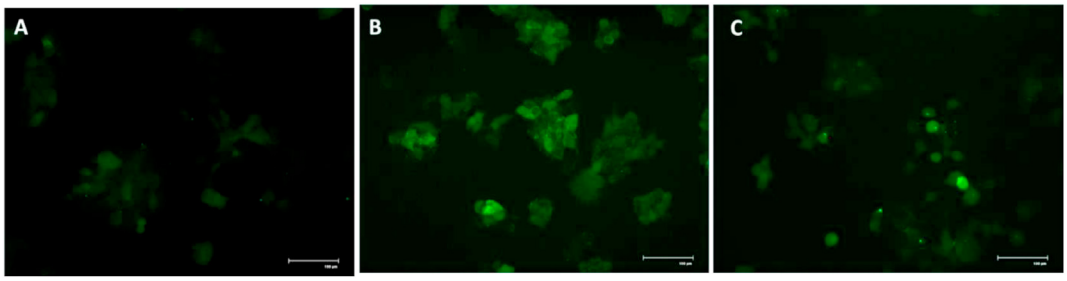

Fig. 7. (a) Detection of intracellular ROS production in MCF-7 cells. (**A**) Least amount of ROS generated in untreated cells which is a basic feature of cancer cells (**B**) H_2O_2 (0.05%) used as a positive control and acts as a ROS inducing agent (**C**) The cells were treated with compound **8f** of desired concentration for 48 h. The fluorescence intensity of DCFHDA was also found increased in 3.5 μM concentration of compound **8f** after treatment.

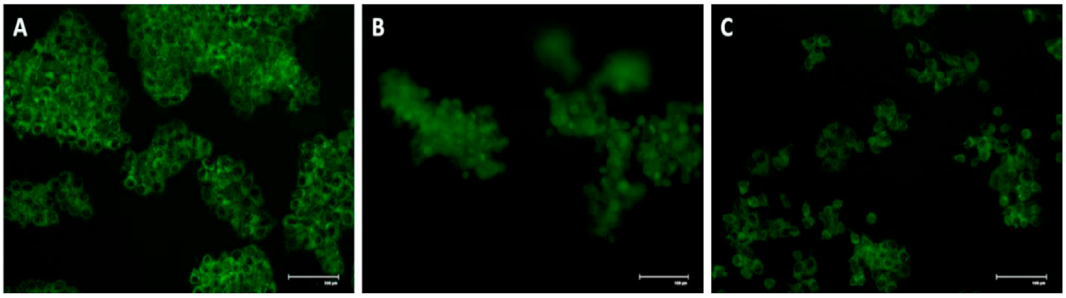

Fig. 8. Loss of MMP of **8f** derivative treated MCF-7 cell lines was determined through rhodamine-123 staining and observed under fluorescence microscope. (**A**) The untreated groups demonstrated intact mitochondria in comparison to the treated groups which prompted a significant decrease in MMP (**B**) tamoxifen treated group (9.5 μM) was taken as standard positive control drug (**C**) represents compound **8f** treated group at 3.5 μM concentration for 48 h.

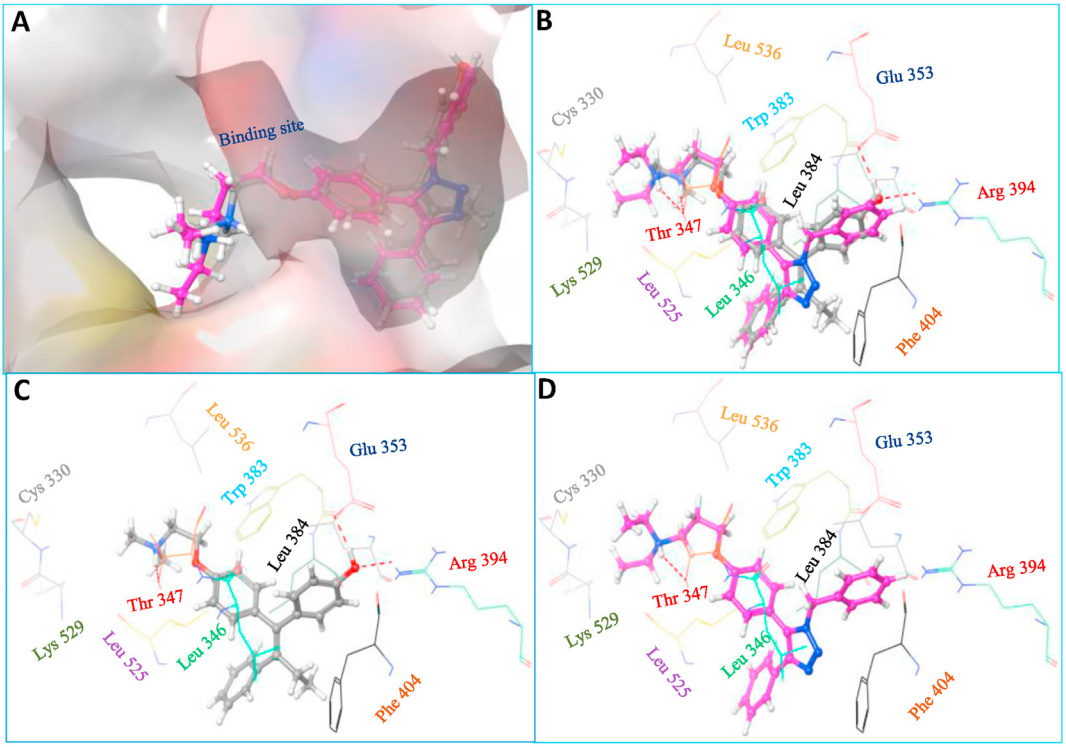

Fig. 9. Interaction of 4-hydroxytamoxifen (grey) and **8f** (purple) with ER-α (PDB: 3ERT). (**A**) Surface view of ER-α protein showing the active site; (**B**) Overlay of 4-hydroxytamoxifen and **8f** in the active site of ER-α; (**C**) Interactions of 4-hydroxytamoxifen with ER-α active site; and (**D**) Interactions of **8f** with ER-α active site

In order to rationalize the activity profile, next we carried out the molecular docking study of computationally energy minimized conformation of active compound **8f** with structurally related drug moiety, 4-hydroxy tamoxifen (OHT) in ER α. Infact, compound **8f** displayed strong binding at the active site with the dock score of −9.97 while the co-crystallized ligand 4-hydroxytamoxifen has a dock score of −13.61. The overlay image of **8f** with 4-hydroxytamoxifen has indicated the perfect alignment of these two ligands with each other as shown in Fig. 9. The N-benzyl and phenyl ring of **8f** were precisely superimposed over phenolic and phenyl ring of 4-hydroxytamoxifen, respectively and the triazole moiety of **8f** occupied the junction of three aryl rings containing C=C bond. The key H-bonding interaction with Thr-347 of 4-hydroxytamoxifen was also observed in **8f**. The favorable interaction of **8f** with ER-α may be indicating that modulation of ER-α activity could be its possible mode of anticancer action.

3. Conclusion

In this research work, we have synthesized triaryl-substituted 1,2,3-triazoles in order to check cytotoxicity on breast and colon cancer cell lines. The biological results indicated that among all the compounds screened against different cell lines, compound **8f** induced apoptosis at IC_{50} dose chosen at 3.5 μM concentration in MCF-7 cells. Moreover, this diethyl amine substituted **8f** molecule inhibited cell proliferation effectively in both breast and colon cancer cell line variants. As per the screening of **8f** against normal breast epithelial cell line FR-2, the study observed the lack of cytotoxic effect at 3.5 μM concentration nearly indicating it to be 10-fold safer from their IC_{50} value against MCF-7 cells and far better than the tamoxifen. The mechanistic studies revealed that the compound **8f** triggered apoptosis in breast cancer cells which is a mechanism of autolysis of cells. Therefore, this work displays an important prospective towards futuristic

approaches and possibilities for target molecule **8f** as a suitable chemotherapeutic agent.

4. Experimental section

4.1. Chemistry

General Information ^{1}H and ^{13}C NMR spectra in $CDCl_3$ and CD_3OD were recorded on Bruker Avance III-400 MHz, using $(CH_3)_4Si$ as an internal standard. Chemical shifts (δ) are expressed in parts per million referenced to the residual solvent (i.e., ^{1}H 7.24 ppm, ^{13}C 77.1 ppm for $CDCl_3$; ^{1}H 3.35, 4.78 ppm, ^{13}C 49.3 ppm for CD_3OD). Signal multiplicity is expressed as follows: s (singlet), br s (broad singlet), d (doublet), t (triplet), q (quartet), m (multiplet). *J* values are given in hertz (Hz). For the HRMS measurement, Q-TOF was used. All reactions and purity of the synthesized compounds were monitored by TLC using silica gel 60 F254 aluminium plates. Visualization was accomplished by UV light, exposure to iodine vapours and by treating the plates with dragendorff reagent followed by heating. Unless otherwise indicated, materials and solvents were purchased and used without further purification.

4.1.1. General procedure for the synthesis of iodo-triazoles (3a-3d, 4)

A suspension of phenylacetylene **1** (500 mg, 4.89 mmol, 1.0 equiv.) and iodine (1.86 g, 7.33 mmol, 1.5 equiv.) was added to a mixture of CuI (91 mg, 10 mol %) and β−cyclodextrin (46 mg, 1.0 mol %) dissolved in water (20 mL) and stirred for 30 min at room temperature. A red homogeneous solution was formed, which confirmed the formation of 1-iodophenylacetylene as revealed by TLC analysis. Thereafter, benzyl bromide **2** (581 μL, 4.89 mmol, 1.0 equiv.), sodium azide (636 mg, 9.78 mmol, 2.0 equiv.) and triethylamine (205 μL, 1.46 mmol, 0.3 equiv.) were added to the reaction mixture and reaction temperature was raised up to 90 °C for 4 h. After completion of reaction as monitored by TLC, the reaction mixture was diluted with water (20 mL). The aqueous solution was extracted with EtOAc (3 × 10 mL) and combined organic layer was washed with saturated $Na_2S_2O_3$ solution, dried over anhydrous Na_2SO_4, and evaporated in vacuum. The residue was purified by column chromatography using (10% EtOAc: petroleum ether) to afford the desired product.

4.1.1.1. 1-Benzyl-5-iodo-4-phenyl-1H-1,2,3-triazole (3a). Yield: 79% (1.23 g), white solid; M. p.: 138−140 °C; ^{1}H NMR (400 MHz, $CDCl_3$) δ 7.87 (d, *J* = 8.4 Hz, 2H), 7.40−7.36 (m, 2H), 7.28−7.26 (m, 6H), 5.60 (s, 2H); ^{13}C NMR (125 MHz, $CDCl_3$) δ 150.23 (C), 134.30(C), 130.21 (C), 128.94 (2CH), 128.63 (CH), 128.56 (2CH), 128.52 (CH), 127.83 (2CH), 127.46 (2CH), 76.45 (C), 54.42 (CH_2); HRMS [ESI]: *m/z* calculated for $C_{15}H_{12}IN_3$ $[M+H]^+$ 362.0109, found: 362.0129.

4.1.1.2. 5-Iodo-1-(4-methoxybenzyl)-4-phenyl-1H-1,2,3-triazole (3 b). Yield: 72% (1.38 g), off-white solid; M. p.: 115−117 °C; ^{1}H NMR (400 MHz, $CDCl_3$) δ 7.90−7.82 (m, 2H), 7.43−7.28 (m, 3H), 7.22 (d, *J* = 8.6 Hz, 2H), 6.81 (d, *J* = 8.7 Hz, 2H), 5.53 (s, 2H), 3.72 (s, 3H); ^{13}C NMR (101 MHz, $CDCl_3$) δ 159.79 (C), 150.19 (C), 130.32 (C), 129.43 (2CH), 128.56 (CH), 128.51 (2CH), 127.49 (2CH), 126.45 (C), 114.30 (2CH), 76.03 (C), 55.31 (OCH_3), 54.00 (CH_2) ppm; HRMS (ESI): calcd. for $C_{16}H_{14}IN_3O$ $[M+H]^+$, 392.0215; found: 392.0254.

4.1.1.3. 1-Benzyl-5-iodo-4-(4-methoxyphenyl)-1H-1,2,3-triazole (3c). Yield: 80% (1.18 g), off-white solid; M. p.: 107−109 °C; ^{1}H NMR (400 MHz, $CDCl_3$) δ 7.91−7.84 (m, 2H), 7.33 (ddd, *J* = 11.2, 8.5, 6.7 Hz, 5H), 7.03−6.95 (m, 2H), 5.66 (s, 2H), 3.85 (s, 3H); ^{13}C NMR (101 MHz, $CDCl_3$) δ 159.95 (C), 150.18 (C), 134.46 (C), 128.90 (2CH), 128.82 (2CH), 128.46 (CH), 127.82 (2CH), 122.80 (C), 113.99 (2CH), 75.63 (C), 55.33 (OCH_3), 54.38 (CH_2) ppm; HRMS (ESI): calcd. for $C_{16}H_{14}IN_3O$ $[M+H]^+$, 392.0215; found: 392.0254.

4.1.1.4. 5-Iodo-1-(4-methoxybenzyl)-4-(4-methoxyphenyl)-1H-1,2,3-triazole (3d). Yield: 85% (1.35 g), yellow solid; M. p.: 126−127 °C; ^{1}H NMR (400 MHz, $CDCl_3$) δ 7.85 (d, *J* = 8.9, 2H), 7.28 (d, *J* = 8.7, 2H), 6.97 (d, *J* = 8.9, 2H), 6.87 (d, *J* = 8.7, 2H), 5.57 (s, 2H), 3.84 (s, 3H), 3.78 (s, 3H);^{13}C NMR (101 MHz, $CDCl_3$) δ 159.92 (C), 159.76 (C), 150.10 (C), 129.42 (2CH), 128.82 (2CH), 126.53 (C), 122.87 (C), 114.28 (2CH), 113.98 (2CH), 75.38 (C), 55.32 (2OCH_3), 53.95 (CH_2) ppm; HRMS (ESI): calcd. for $C_{17}H_{16}IN_3O_2$ $[M+H]^+$, 422.0321; found: 422.0370.

4.1.1.5. 1-Benzyl-4-phenyl-1H-1,2,3-triazole (4). Yield: 20% (230 mg), white solid; M. p.: 135−137 °C;^{1}H NMR (400 MHz, $CDCl_3$) δ 7.81−7.78 (m, 2H), 7.66 (s, 1H), 7.41−7.36 (m, 5H), 7.33−7.30(m, 3H), 5.57 (s, 2H); ^{13}C NMR (101 MHz, $CDCl_3$) δ 148.26 (C), 134.72 (C), 130.58 (C), 129.16 (2CH), 128.79 (3CH), 128.15 (CH), 128.06 (2CH), 125.72 (2CH), 119.45 (CH), 54.24 (CH_2); HRMS [ESI]: *m/z* calculated for $C_{15}H_{13}N_3$ $[M+H]^+$ 236.1143, found: 236.1189.

4.1.1.6. 4-Bromophenyl 4-methylbenzenesulfonate. To a solution of 4-bromophenol (400 mg, 2.30 mmol, 1.0 equiv.) in DCM (2 mL) at 0 °C were added tosyl chloride (485 mg, 2.54 mmol, 1.1 equiv.) portion-wise and pyridine (205 μL, 2.54 mmol, 1.1 equiv.) dropwise. The reaction mixture was warmed to room temperature and stirred for 4 h. Distilled water (20 mL) and saturated aqueous NH_4Cl (10 mL) were added, and the mixture was extracted with CH_2Cl_2 (3 × 60 mL). The combined organic fractions were washed with brine, dried (Na_2SO_4), and concentrated in vacuo. The purification of the crude material was thus obtained by flash chromatography (silica gel, 10% EtOAc in n-hexane) afforded bromobenzene tosylate as a white solid. Yield: 85% (644 mg); M. p.: 77−78 °C; ^{1}H NMR (400 MHz, $CDCl_3$) δ 7.72(d, *J* = 8.4 Hz, 2H), 7.43 (d, *J* = 8.9 Hz, 2H), 7.35(d, *J* = 8.1 Hz, 2H), 6.89 (d, *J* = 6.8 Hz, 2H), 2.48 (s, 3H); ^{13}C NMR (101 MHz, $CDCl_3$) δ 148.66 (C), 145.60 (C), 132.71 (2CH), 132.18 (C), 129.84 (2CH), 128.53 (2CH), 124.14 (2CH), 120.54 (C), 21.69 (CH_3) ppm; HRMS (ESI): calcd. for $C_{13}H_{11}BrO_3S$ $[M+H]^+$, 328.9625; found: 328.1437.

4.1.1.7. 4-(1-Benzyl-4-phenyl-1H-1,2,3-triazol-5-yl)phenyl 4-methylbenzenesulfonate (5). A suspension of $Pd(OAc)_2$ (8.0 mg, 4.0 mol%), PCy_3 (19 mg, 8.0 mol%), K_2CO_3 (235 mg, 1.69 mmol, 2 equiv.), **4** (200 mg, 0.85 mmol, 1 equiv.) and 4-bromophenyl 4-methylbenzenesulfonate (415 mg, 1.27 mmol, 1.50 equiv.) in toluene (2 mL) was stirred under N_2 for 24 h at 120 °C. Reaction was quenched with cold water and extracted with Et_2O (2 × 50 mL). The combined organic layers were washed with aqueous NH_4Cl (50 mL), H_2O (50 mL) and brine (50 mL), dried over Na_2SO_4 and concentrated in vacuum. The remaining residue was purified by column chromatography (silica gel, 50% EtOAc in n-hexane) to afford (**5**) as an off-white solid. Yield: 75% (307 mg); M. p.: 103−105 °C; ^{1}H NMR (400 MHz, $CDCl_3$) δ 7.73(d, *J* = 8.4 Hz, 2H), 7.49−7.44 (m, 2H), 7.33(d, *J* = 8.0 Hz, 2H), 7.26−7.23 (m, 6H), 7.05 (s, 4H), 6.96 (dd, *J* = 7.5, 1.9 Hz, 2H), 5.38 (s, 2H), 2.46 (s, 3H); ^{13}C NMR (101 MHz, $CDCl_3$) δ 150.48 (C), 145.76 (C), 144.91 (C), 135.07 (C), 132.48 (C), 132.25 (C), 131.56 (2CH), 130.58 (C), 129.84 (2CH), 128.79 (2CH), 128.51 (2CH), 128.47 (2CH), 128.31 (CH), 127.92 (CH), 127.42 (2CH), 126.85 (C), 126.75 (2CH), 123.27 (2CH), 52.28 (CH_2), 21.74 (CH_3) ppm; HRMS (ESI): calcd. for $C_{28}H_{23}N_3O_3S$ $[M+H]^+$, 482.1494; found: 482.1534.

4.1.2. General procedure for Suzuki reactions (6a-6e)

A mixture of **3a** (500 mg, 1.38 mmol, 1 equiv.), phenylboronic acid (287 mg, 2.07 mmol, 1.5 equiv.), K_2CO_3 (476 mg, 3.45 mmol, 2.5

equiv.), and $Pd(PPh_3)_2Cl_2$ (97 mg, 0.13 mmol, 0.1 equiv.) in DMF:H_2O (2.5:0.5, 6 mL) was stirred for 4 h at 80 °C. Then the resultant mixture was poured into H_2O (15 mL) and was extracted with CH_2Cl_2 (3 × 15 mL). The combined organic layers were washed with brine (15 mL) and dried over Na_2SO_4. The solvent was removed under vacuum, and the residue was purified by column chromatography [silica gel, 30% EtOAc in petroleum ether] to give (**6a-6e**);

4.1.2.1. 4-(1-Benzyl-4-phenyl-1H-1,2,3-triazol-5-yl)phenol (6a). Yield: 85% (385 mg), white solid; M. p.: 180–182 °C; ^{1}H NMR (400 MHz, $CDCl_3$) δ 7.58 (dd, J = 7.8, 1.5 Hz, 2H), 7.28–7.24 (m, 6H), 7.07 (d, J = 3.6 Hz, 2H), 6.98 (q, J = 8.7 Hz, 4H), 5.42 (s, 2H); ^{13}C NMR (101 MHz, $CDCl_3$) δ 157.50 (C), 144.45 (C), 135.36 (C), 134.08 (C), 131.57 (2CH), 130.81 (C), 128.73 (2CH), 128.47 (2CH), 128.17 (CH), 127.75 (CH), 127.53 (2CH), 126.75 (2CH), 119.04 (C), 116.42 (2CH), 52.01 (CH_2) ppm; HRMS (ESI): calcd. for $C_{16}H_{14}IN_3O$ $[M+H]^+$, 328.1405; found: 328.1443.

4.1.2.2. 4-((4,5-Diphenyl-1H-1,2,3-triazol-1-yl)methyl)phenol (6 b). Yield: 80% (335 mg), pale-yellow solid; M. p.: 172–173 °C; ^{1}H NMR (400 MHz, $CDCl_3$) δ 7.58–7.41 (m, 6H), 7.25–7.23 (m, 2H), 7.17 (d, J = 6.8, 2H), 6.90 (d, J = 8.5, 2H), 6.73 (d, J = 8.5, 2H), 5.32 (s, 2H); ^{13}C NMR (101 MHz, $CDCl_3$) δ 155.95 (C), 144.53 (C), 133.84 (C), 130.75 (C), 130.20 (2CH), 129.75 (C), 129.26 (2CH), 129.21 (2CH), 128.49 (2CH), 127.86 (C), 127.78 (C), 127.16 (C), 126.76 (2CH), 115.69 (2CH), 51.69 (CH_2) ppm; HRMS (ESI): calcd. for $C_{21}H_{17}N_3O$ $[M+H]^+$, 328.1405; found: 328.1441.

4.1.2.3. 4-(1-Benzyl-5-phenyl-1H-1,2,3-triazol-4-yl)phenol (6c). Yield: 84% (351 mg); pale-yellow solid; M. p.: 166–168 °C; ^{1}H NMR (400 MHz, $CDCl_3$) δ 7.47–7.38 (m, 5H), 7.26–7.24 (m, 3H), 7.13 (d, J = 6.9, 2H), 7.02 (dd, J = 6.6, 2.8, 2H), 6.73 (d, J = 8.7, 2H), 5.40 (s, 2H); ^{13}C NMR (101 MHz, $CDCl_3$) δ 155.70 (C), 144.53 (C), 135.37 (C), 133.17 (C), 130.18 (2CH), 129.63 (CH), 129.16 (2CH), 128.71 (2CH), 128.32 (2CH), 128.16 (CH), 127.92 (C), 127.52 (2CH), 123.27 (C), 115.53 (2CH), 52.11 (CH_2) ppm; HRMS (ESI): calcd. for $C_{21}H_{17}N_3O$ $[M+H]^+$, 328.1405; found: 328.1414.

4.1.2.4. 4-(1-(4-Methoxybenzyl)-4-(4-methoxyphenyl)-1H-1,2,3-triazol-5-yl)phenol (6d). Yield: 88% (404 mg), yellow solid; M. p.: 127–129 °C; ^{1}H NMR (400 MHz, $CDCl_3$) δ 7.49 (d, J = 8.9, 2H), 6.99 (d, J = 9.1, 6H), 6.78 (dd, J = 12.2, 8.8, 4H), 5.33 (s, 2H), 3.76 (d, J = 4.2, 6H);^{13}C NMR (101 MHz, $CDCl_3$) δ 159.47 (C), 159.22 (C), 157.75 (C), 144.30 (C), 133.22 (C), 131.62 (2CH), 129.11 (2CH), 128.05 (2CH), 127.52 (C), 123.54 (C), 119.02 (C), 116.45 (2CH), 114.07 (2CH), 113.94 (2CH), 55.28 (OCH_3), 55.21 (OCH_3), 51.55 (CH_2). ppm; HRMS (ESI): calcd. for $C_{23}H_{21}N_3O_3$ $[M+H]^+$, 388.1616; found: 388.1657.

4.1.2.5. Synthesis of 4-(5-(4-methoxyphenyl)-4H-1,2,3-triazol-4-yl) phenol (6e). Yield: 30% (21 mg), semi-solid; ^{1}H NMR (400 MHz, $CDCl_3$) δ 7.46 (d, J = 15.1, 4H), 6.88 (d, J = 15.9, 4H), 3.84 (s, 3H); ESI-MS (m/z): 268.25 $[M+H]^+$, 374.35 $[M+H]^+$; HRMS (ESI): calcd. for $C_{15}H_{13}N_3O_2$ $[M+H]^+$, 268.1041; found: 268.1078.

4.1.3. General procedure for the synthesis of desired halide with different aliphatic chains (7a-7f)

Compound **6** (200 mg, 6.11 mmol, 1.0 equiv.) was alkylated with ώ-dihaloalkanes (152 μL, 1.83 mmol, 3.0 equiv.) in the presence of anhydrous K_2CO_3 (337 mg, 2.44 mmol, 4.0 equiv.), in dry acetone (10 mL), was refluxed for 4–5 h. On completion, the reaction mixture was cooled and filtered. The filterate was concenterated and was purified by column chromatography [silica gel, 30% EtOAc in petroleum ether] to give (**7**) as yellow oil.

4.1.3.1. 1-Benzyl-5-(4-(2-chloroethoxy)phenyl)-4-phenyl-1H-1,2,3-triazole (7a). Yield: 85% (183 mg); ^{1}H NMR (400 MHz, $CDCl_3$) δ 7.57 (dd, J = 8.0, 1.5 Hz, 2H), 7.27–7.21 (m, 6H), 7.05 (dd, J = 7.4, 5.3 Hz, 4H), 6.94 (d, J = 8.7 Hz, 2H), 5.38 (s, 2H), 4.26 (t, 2H), 3.84 (t, 2H). ^{13}C NMR (101 MHz, $CDCl_3$) δ 159.19 (C), 144.54 (C), 135.50 (C), 133.55 (C), 131.57 (2CH), 131.02 (C), 128.72 (2CH), 128.44 (2CH), 128.14 (CH), 127.67 (CH), 127.44 (2CH), 126.68 (2CH), 120.45 (C), 115.31 (2CH), 68.08 (CH_2), 51.95 (CH_2), 41.76 (CH_2) ppm; HRMS (ESI): calcd. for $C_{23}H_{20}ClN_3O$ $[M+H]^+$, 390.1328; found: 390.1371.

4.1.3.2. 1-Benzyl-5-(4-(3-chloropropoxy)phenyl)-4-phenyl-1H-1,2,3-triazole (7b). Yield: 88% (217 mg); ^{1}H NMR (400 MHz, $CDCl_3$) δ 7.58 (dd, J = 8.1, 1.4 Hz, 2H), 7.24 (dd, J = 5.0, 2.6 Hz, 6H), 7.04 (d, J = 8.8 Hz, 4H), 6.94 (d, J = 8.7 Hz, 2H), 5.38 (s, 2H), 4.14 (t, 2H), 3.75 (t, 2H), 2.28–2.22 (m, 2H). ^{13}C NMR (101 MHz, $CDCl_3$) δ 159.77 (C), 144.44 (C), 135.60 (C), 133.77 (C), 131.49 (2CH), 131.17 (C), 128.72 (2CH), 128.45 (2CH), 128.12 (CH), 127.64 (CH), 127.47 (2CH), 126.69 (2CH), 119.88 (C), 115.23 (2CH), 64.50 (CH_2), 51.90 (CH_2), 41.41 (CH_2), 32.21 (CH_2) ppm; HRMS (ESI): calcd. for $C_{24}H_{22}ClN_3O$ $[M+H]^+$, 404.1485; found: 404.1524.

4.1.3.3. 1-Benzyl-5-(4-(4-chlorobutoxy)phenyl)-4-phenyl-1H-1,2,3-triazole (7c). Yield: 90% (229 mg); ^{1}H NMR (400 MHz, $CDCl_3$) δ 7.60 (dd, J = 8.1, 1.5 Hz, 2H), 7.25 (dt, J = 8.9, 5.1 Hz, 6H), 7.10–7.01 (m, 4H), 6.92 (d, J = 8.8 Hz, 2H), 5.39 (s, 2H), 4.04 (t, 2H), 3.64 (t, 2H), 2.07–1.95 (m, 4H); ^{13}C NMR (126 MHz, $CDCl_3$) δ 159.85 (C), 144.45 (C), 135.56 (C), 133.77 (C), 131.46 (2CH), 131.08 (C), 128.73 (2CH), 128.45 (2CH), 128.13 (CH), 127.64 (CH), 127.47 (2CH), 126.66 (2CH), 119.62 (C), 115.09 (2CH), 67.13 (CH_2), 51.89 (CH_2), 44.74 (CH_2), 29.30 (CH_2), 26.61 (CH_2) ppm; HRMS (ESI): calcd. for $C_{25}H_{24}ClN_3O$ $[M+H]^+$, 418.1641; found: 418.1683.

4.1.3.4. 1-Benzyl-5-(4-((5-chloropentyl)oxy)phenyl)-4-phenyl-1H-1,2,3-triazole (7d). Yield: 92% (242 mg); ^{1}H NMR (400 MHz, $CDCl_3$) δ 7.58 (dd, J = 8.1, 1.6 Hz, 2H), 7.26 (t, 6H), 7.04 (d, J = 8.7 Hz, 4H), 6.91 (d, J = 8.8 Hz, 2H), 5.39 (s, 2H), 4.02 (t, 2H), 3.59 (t, 2H), 1.93–1.82 (m, 4H), 1.67 (dd, J = 13.0, 5.8 Hz, 2H). ^{13}C NMR (126 MHz, $CDCl_3$) δ 159.99 (C), 144.45 (C), 135.59 (C), 133.79 (C), 131.43 (2CH), 131.13 (C), 128.70 (2CH), 128.41 (2CH), 128.10 (CH), 127.59 (CH), 127.47 (2CH), 126.66 (2CH), 119.56 (C), 115.11 (2CH), 67.76 (CH_2), 51.87 (CH_2), 44.83 (CH_2), 32.30 (CH_2), 28.53 (CH_2), 23.56 (CH_2) ppm; HRMS (ESI): calcd. for $C_{26}H_{26}ClN_3O$ $[M+H]^+$, 432.1798; found: 432.1822.

4.1.3.5. 1-(4-(3-Chloropropoxy)benzyl)-4,5-diphenyl-1H-1,2,3-triazole (7e). Yield: 87% (214 mg); ^{1}H NMR (400 MHz, $CDCl_3$) δ 7.54 (dd, J = 7.7, 1.8, 2H), 7.47 (dd, J = 14.3, 7.3, 2H), 7.26–7.23 (m, 4H), 7.16 (d, J = 6.8, 2H), 6.96 (d, J = 8.6, 2H), 6.77 (d, J = 8.7, 2H), 5.34 (s, 2H), 4.07 (t, 2H), 3.73 (t, 2H), 2.24–2.18 (m, 2H); ^{13}C NMR (101 MHz, $CDCl_3$) δ 158.61 (C), 144.55 (C), 133.70 (C), 130.99 (C), 130.19 (2CH), 129.67 (CH), 129.18 (2CH), 129.10 (2CH), 128.43 (2CH), 128.04 (C), 127.72 (C), 127.67 (CH), 126.73 (2CH), 114.65 (2CH), 64.35 (CH_2), 51.59 (CH_2), 41.43 (CH_2), 32.22 (CH_2) ppm; HRMS (ESI): calcd. for $C_{24}H_{22}ClN_3O$ $[M+H]^+$, 404.1485; found: 404.1519.

4.1.3.6. 5-(4-(3-Chloropropoxy)phenyl)-1-(4-methoxybenzyl)-4-(4-methoxyphenyl)-1H-1,2,3-triazole (7f). Yield: 91% (217 mg); ^{1}H NMR (400 MHz, $CDCl_3$) δ 7.48 (d, J = 8.8, 2H), 7.06 (d, J = 8.7, 2H), 6.97 (dd, J = 18.1, 8.6, 4H), 6.79 (dd, J = 8.7, 7.1, 4H), 5.31 (s, 2H), 4.17 (t, 2H), 3.80 (d, J = 6.3, 2H), 3.77 (s, 6H), 2.33–2.24 (m, 2H);^{13}C NMR (126 MHz, $CDCl_3$) δ 159.61 (C), 159.38 (C), 159.11 (C), 144.36 (C), 132.74 (C), 131.57 (2CH), 129.00 (2CH), 127.96 (2CH), 127.64 (C), 123.71 (C), 120.08 (C), 115.10 (2CH), 114.01 (2CH), 113.87 (2CH), 64.32 (CH_2), 55.29 (OCH_3), 55.21 (OCH_3), 51.45 (CH_2), 41.47 (CH_2), 32.17 (CH_2) ppm; HRMS (ESI): calcd. for $C_{26}H_{26}ClN_3O_3$ $[M+H]^+$,

464.1696; found: 464.1743.

4.1.4. General procedure for amination (8a-8p)

A solution of **7a** (100 mg, 0.25 mmol, 1.0 equiv.), piperidine (101 μL, 1.02 mmol, 4.0 equiv.), and tetrabutylammonium iodide (92 mg, 0.25 mmol, 1.0 equiv.) in dry DMF (1.5 mL) was heated at 70–75 °C with stirring for 7 h. The reaction mixture was diluted with ethyl acetate, washed with water, dried over sodium sulphate and concentrated. The concentrate was chromatographed on basic alumina using 10% MeOH/DCM obtained as light-brown oil.

4.1.4.1. 1-(2-(4-(1-Benzyl-4-phenyl-1H-1,2,3-triazol-5-yl)phenoxy) ethyl)piperidine (8a). Yield: 70% (79 mg); ^{1}H NMR (400 MHz, $CDCl_3$) δ 7.57 (dd, J = 8.1, 1.6, 2H), 7.28–7.24 (m, 6H), 7.07–7.02 (m, 4H), 6.95–6.91 (m, 2H), 5.39 (s, 2H), 4.17 (t, 2H), 2.85 (t, 2H), 2.58 (s, 4H), 1.68–1.63 (m, 4H), 1.51–1.47 (m, 2H); ^{13}C NMR (101 MHz, $CDCl_3$) δ 159.80 (C), 144.49 (C), 135.60 (C), 133.77 (C), 131.44 (2CH), 131.15 (C), 128.73 (2CH), 128.44 (2CH), 128.13 (CH), 127.62 (CH), 127.50 (2CH) 126.69 (2CH), 119.77 (C), 115.30 (2CH), 66.09 (CH_2), 57.83 (CH_2), 55.14 ($2CH_2$), 51.93 (CH_2), 25.78 ($2CH_2$), 24.07 (CH_2) ppm. HRMS (ESI): calcd. for $C_{28}H_{30}N_4O$ [M+H]$^+$, 439.2498; found: 439.2489.

4.1.4.2. 1-Benzyl-4-phenyl-5-(4-(2-(pyrrolidin-1-yl)ethoxy)phenyl)-1H-1,2,3-triazole (8b). Yield: 72% (78 mg); ^{1}H NMR (400 MHz, $CDCl_3$) δ 7.57 (dd, J = 8.0, 1.5, 2H), 7.29–7.23 (m, 6H), 7.06–7.03 (m, 4H), 6.94 (d, J = 8.8, 2H), 5.39 (s, 2H), 4.24 (t, 2H), 3.08 (t, 2H), 2.84 (s, 4H), 1.93–1.90 (m, 3H); ^{13}C NMR (101 MHz, $CDCl_3$) δ 159.55 (C), 144.51 (C), 135.57 (C), 133.68 (C), 131.49 (2CH), 131.13 (CH), 128.72 (2CH), 128.42 (2CH), 128.12 (CH), 127.61 (CH), 127.48 (2CH), 126.68 (2CH), 120.05 (C), 115.28 (2CH), 66.52 (CH_2), 54.84 (CH_2), 54.78 ($2CH_2$), 51.92 (CH_2), 23.50 ($2CH_2$) ppm; HRMS (ESI): calcd. for $C_{27}H_{28}N_4O$ [M+H]$^+$, 425.2297; found: 425.2342.

4.1.4.3. 4-(2-(4-(1-Benzyl-4-phenyl-1H-1,2,3-triazol-5-yl)phenoxy) ethyl)morpholine (8c). Yield: 67% (75 mg); ^{1}H NMR (400 MHz, $CDCl_3$) δ 7.57 (dd, J = 8.0, 1.6, 2H), 7.28–7.24 (m, 6H), 7.05 (d, J = 8.7, 4H), 6.93 (d, J = 8.8, 2H), 5.39 (s, 2H), 4.16 (t, 2H), 3.76 (t, 4H), 2.85 (t, 2H), 2.62 (t, 4H); ^{13}C NMR (101 MHz, $CDCl_3$) δ 159.75 (C), 144.51 (C), 135.61 (C), 133.69 (C), 131.47 (2CH), 131.17 (C), 128.69 (2CH), 128.39 (2CH), 128.10 (CH), 127.60 (CH), 127.46 (2CH), 126.70 (2CH), 119.97 (C), 115.28 (2CH), 66.91 ($2CH_2$), 66.07 (CH_2), 57.62 (CH_2), 54.18 ($2CH_2$), 51.90 (CH_2) ppm; HRMS (ESI): calcd. for $C_{27}H_{28}N_4O_2$ [M+H]$^+$, 441.2246; found: 441.2294.

4.1.4.4. 2-(4-(1-Benzyl-4-phenyl-1H-1,2,3-triazol-5-yl)phenoxy)-N,N-diethylethanamine (8d). Yield: 71% (77 mg); ^{1}H NMR (400 MHz, $CDCl_3$) δ 7.57 (dd, J = 8.0, 1.6, 2H), 7.28–7.23 (m, 6H), 7.05 (d, J = 8.7, 4H), 6.93 (d, J = 8.8, 2H), 5.39 (s, 2H), 4.20 (t, 2H), 3.06 (t, 2H), 2.83 (q, J = 7.1, 4H), 1.18 (t, 6H); ^{13}C NMR (101 MHz, $CDCl_3$) δ 159.49 (C), 144.52 (C), 135.57 (C), 133.67 (C), 131.50 (2CH), 131.13 (C), 128.72 (2CH), 128.42 (2CH), 128.12 (CH), 127.61 (CH), 127.47 (2CH), 126.68 (2CH), 120.07 (C), 115.25 (2CH), 65.96 (CH_2), 51.93 (CH_2), 51.60 (CH_2), 47.89 ($2CH_2$), 11.06 ($2CH_3$) ppm; HRMS (ESI): calcd. for $C_{27}H_{30}N_4O$ [M+H]$^+$, 427.2453; found: 427.2489.

4.1.4.5. 1-Benzyl-4-phenyl-5-(4-(3-(pyrrolidin-1-yl)propoxy) phenyl)-1H-1,2,3-triazole (8e). Yield: 73% (79 mg); ^{1}H NMR (400 MHz, $CDCl_3$) δ 7.56 (dd, J = 8.0, 1.6, 2H), 7.27–7.22 (m, 6H), 7.05 (d, J = 8.8, 4H), 6.91 (d, J = 8.7, 2H), 5.39 (s, 2H), 4.13 (t, 2H), 3.19 (t, 4H), 2.42–2.35 (m, 2H), 2.12 (t, 2H); ^{13}C NMR (101 MHz, $CDCl_3$) δ 159.35 (C), 144.52 (C), 135.54 (C), 133.61 (C), 131.57 (2CH), 131.12 (C), 128.73 (2CH), 128.42 (2CH), 128.14 (CH), 127.63 (CH), 127.45 (2CH), 126.70 (2CH), 120.29 (C), 115.17 (2CH), 65.24 (CH_2), 53.98 ($2CH_2$), 53.08 (CH_2), 51.93 (CH_2), 26.18 (CH_2), 23.45 ($2CH_2$) ppm; HRMS (ESI): calcd. for $C_{28}H_{30}N_4O$ [M+H]$^+$, 439.2453; found: 439.2496.

4.1.4.6. 3-(4-(1-Benzyl-4-phenyl-1H-1,2,3-triazol-5-yl)phenoxy)-N,N-diethylpropan-1-amine (8f). Yield: 70% (76 mg); ^{1}H NMR (400 MHz, $CDCl_3$) δ 7.56 (dd, J = 8.0, 1.6, 2H), 7.28–7.21 (m, 6H), 7.05 (d, J = 8.7, 4H), 6.91 (d, J = 8.7, 2H), 5.39 (s, 2H), 4.11 (t, 2H), 3.05 (t, 2H), 2.98 (q, J = 7.2, 4H), 2.28–2.21 (m, 2H), 1.31 (t, 6H); ^{13}C NMR (101 MHz, $CDCl_3$) δ 159.53 (C), 144.50 (C), 135.55 (C), 133.67 (C), 131.53 (2CH), 131.11 (C), 128.73 (2CH), 128.43 (2CH), 128.14 (CH), 127.64 (CH), 127.45 (2CH), 126.69 (2CH), 120.06 (C), 115.16 (2CH), 65.59 (CH_2), 51.93 (CH_2), 49.30 (CH_2), 47.02 ($2CH_2$), 25.02 (CH_2), 9.81 ($2CH_3$) ppm; HRMS (ESI): calcd. for $C_{28}H_{32}N_4O$ [M+H]$^+$, 441.2610; found: 441.2647.

4.1.4.7. 1-(3-(4-(1-Benzyl-4-phenyl-1H-1,2,3-triazol-5-yl)phenoxy) propyl)piperidine (8g). Yield: 71% (79 mg); ^{1}H NMR (400 MHz, $CDCl_3$) δ7.57 (dd, J = 8.0, 1.6, 2H), 7.28–7.23 (m, 6H), 7.07–7.02 (m, 4H), 6.91 (d, J = 8.7, 2H), 5.39 (s, 2H), 4.07 (t, 2H), 2.65 (t, 2H), 2.57 (s, 4H), 2.14–2.07 (m, 2H), 1.73–1.68 (m, 4H), 1.50 (t, 2H); ^{13}C NMR (101 MHz, $CDCl_3$) δ 160.04 (C), 144.44 (C), 135.62 (C), 133.82 (C), 131.41 (2CH), 131.19 (C), 128.70 (2CH), 128.41 (2CH), 128.09 (CH), 127.58 (CH), 127.48 (2CH), 126.67 (2CH), 119.56 (C), 115.21 (2CH), 66.57 (CH_2), 55.82 (CH_2), 54.58 ($2CH_2$), 51.88 (CH_2), 26.56 (CH_2), 25.70 ($2CH_2$), 24.24 (CH_2) ppm; HRMS (ESI): calcd. for $C_{29}H_{32}N_4O$ [M+H]$^+$, 453.2610; found: 453.2661.

4.1.4.8. 4-(3-(4-(1-Benzyl-4-phenyl-1H-1,2,3-triazol-5-yl)phenoxy) propyl)morpholine (8h). Yield: 69% (78 mg); ^{1}H NMR (400 MHz, $CDCl_3$) δ 7.57 (dd, J = 7.9, 1.5, 2H), 7.27–7.24 (m, 6H), 7.07–7.03 (m, 4H), 6.92 (d, J = 8.7, 2H), 5.39 (s, 2H), 4.07 (t, 2H), 3.73 (t, 4H), 2.56 (t, 2H), 2.50 (s, 4H), 2.05–1.98 (m, 2H); ^{13}C NMR (101 MHz, $CDCl_3$) δ 160.01 (C), 144.46 (C), 135.61 (C), 133.79 (C), 131.44 (2CH), 131.16 (C), 128.71 (2CH), 128.41 (2CH), 128.10 (CH), 127.60 (CH), 127.46 (2CH), 126.69 (2CH), 119.62 (C), 115.17 (2CH), 66.94 ($2CH_2$), 66.30 (CH_2), 55.52 (CH_2), 53.76 ($2CH_2$), 51.87 ($2CH_2$), 26.38 (CH_2) ppm; HRMS (ESI): calcd. for $C_{28}H_{30}N_4O_2$ [M+H]$^+$, 455.2402; found: 455.2446.

4.1.4.9. 1-Benzyl-4-phenyl-5-(4-(4-(pyrrolidin-1-yl)butoxy)phenyl)-1H-1,2,3-triazole (8i). Yield: 70% (75 mg); ^{1}H NMR (400 MHz, $CDCl_3$) δ 7.57 (dd, J = 8.0, 1.5, 2H), 7.28–7.24 (m, 6H), 7.07–7.03 (m, 4H), 6.90 (d, J = 8.7, 2H), 5.39 (s, 2H), 4.05 (t, 2H), 3.31 (s, 4H), 3.18–3.14 (m, 2H), 2.18 (t, 6H), 1.927–1.90 (m, 4H); ^{13}C NMR (101 MHz, $CDCl_3$) δ 159.60 (C), 144.50 (C), 135.58 (C), 133.68 (C), 131.54 (2CH), 131.14 (C), 128.74 (2CH), 128.43 (2CH), 128.14 (CH), 127.63 (CH), 127.46 (2CH), 126.70 (2CH), 120.02 (C), 115.13 (2CH), 67.01 (CH_2), 55.43 (CH_2), 53.77 ($2CH_2$), 51.91 (CH_2), 26.78 (CH_2), 23.41 ($2CH_2$), 22.98 (CH_2) ppm; HRMS (ESI): calcd. for $C_{29}H_{32}N_4O$ [M+H]$^+$, 453.2610; found: 453.2649.

4.1.4.10. 4-(4-(1-Benzyl-4-phenyl-1H-1,2,3-triazol-5-yl)phenoxy)-N,N-diethylbutan-1-amine (8j). Yield: 71% (77 mg); ^{1}H NMR (400 MHz, $CDCl_3$) δ 7.57 (dd, J = 8.0, 1.5, 2H), 7.28–7.24 (m, 6H), 7.07–7.04 (m, 4H), 6.90 (d, J = 8.7, 2H), 5.40 (s, 2H), 4.05 (t, 2H), 3.16 (q, J = 7.3, 4H), 3.09 (t, 2H), 2.12–2.04 (m, 2H), 1.95–1.88 (m, 2H), 1.41 (t, 6H); ^{13}C NMR (101 MHz, $CDCl_3$) δ 159.60 (C), 144.50 (C), 135.57 (C), 133.67 (C), 131.55 (2CH), 131.11 (C), 128.73 (2CH), 128.43 (2CH), 128.13 (CH), 127.63 (CH), 127.44 (2CH), 126.69 (2CH), 120.02 (C), 115.08 (2CH), 67.00 (CH_2), 51.91 (CH_2), 51.39 (CH_2), 46.59 ($2CH_2$), 26.64 (CH_2), 20.87 (CH_2), 8.64 ($2CH_3$) ppm; HRMS (ESI): calcd. for $C_{29}H_{34}N_4O$ [M+H]$^+$, 455.2766; found: 455.2804.

4.1.4.11. 1-(4-(4-(1-Benzyl-4-phenyl-1H-1,2,3-triazol-5-yl)phenoxy) butyl)piperidine (8k). Yield: 70% (78 mg); ^{1}H NMR (400 MHz,

$CDCl_3$) δ 7.57 (dd, J = 8.1, 1.5, 2H), 7.28–7.24 (m, 6H), 7.05 (dt, J = 4.3, 3.0, 4H), 6.90 (d, J = 8.7, 2H), 5.39 (s, 2H), 4.05 (t, 2H), 3.01 (dd, J = 25.2, 17.0, 6H), 2.20–2.03 (m, 6H), 1.93–1.86 (m, 2H), 1.70 (s, 2H); ^{13}C NMR (101 MHz, $CDCl_3$) δ 159.66 (C), 144.52 (C), 135.60 (C), 133.71 (C), 131.56 (2CH), 131.15 (C), 128.76 (2CH), 128.45 (2CH), 128.15 (CH), 127.64 (CH), 127.48 (2CH), 126.72 (2CH), 120.01 (C), 115.14 (2CH), 67.11 (CH_2), 57.44 (CH_2), 53.43 ($2CH_2$), 51.93 (CH_2), 26.80 (CH_2), 22.80 ($2CH_2$), 22.31 (CH_2) ppm; HRMS (ESI): calcd. for $C_{30}H_{34}N_4O$ $[M+H]^+$, 467.2766; found: 467.2810.

4.1.4.12. 4-(4-(4-(1-Benzyl-4-phenyl-1H-1,2,3-triazol-5-yl)phenoxy) butyl)morpholine (8l). Yield: 68% (76 mg); ^{1}H NMR (400 MHz, $CDCl_3$) δ ^{1}H NMR (400 MHz, $CDCl_3$) δ 7.57 (dd, J = 8.0, 1.5, 2H), 7.28–7.24 (m, 6H), 7.07–7.03 (m, 4H), 6.91 (d, J = 8.7, 2H), 5.39 (s, 2H), 4.03 (t, 2H), 3.72 (t, 4H), 2.49–2.42 (m, 6H), 1.89–1.83 (m, 2H), 1.75–1.69 (m, 2H); ^{13}C NMR (101 MHz, $CDCl_3$) δ 160.06 (C), 144.46 (C), 135.62 (C), 133.80 (C), 131.44 (2CH), 131.17 (C), 128.70 (2CH), 128.40 (2CH), 128.09 (CH), 127.59 (CH), 127.47 (2CH), 126.69 (2CH), 119.57 (C), 115.13 (2CH), 67.86 (CH_2), 66.92 ($2CH_2$), 58.57 (CH_2), 53.70 ($2CH_2$), 51.88 (CH_2), 27.19 (CH_2), 23.03 (CH_2) ppm; HRMS (ESI): calcd. for $C_{29}H_{32}N_4O_2$ $[M+H]^+$, 469.2559; found: 469.2591.

4.1.4.13. 1-Benzyl-4-phenyl-5-(4-((5-(pyrrolidin-1-yl)pentyl)oxy) phenyl)-1H-1,2,3-triazole (8 m). Yield: 73% (79 mg); ^{1}H NMR (400 MHz, $CDCl_3$) δ 7.58 (dd, J = 8.0, 1.5, 2H), 7.28–7.24 (m, 6H), 7.07–7.04 (m, 4H), 6.90 (d, J = 8.7, 2H), 5.39 (s, 2H), 4.01 (t, 2H), 3.31 (s, 4H), 3.10 (t, 2H), 2.18 (s, 4H), 2.05–2.01 (m, 2H), 1.90–1.86 (m, 2H), 1.64–1.60 (m, 2H); ^{13}C NMR (101 MHz, $CDCl_3$) δ 159.88 (C), 144.45 (C), 135.59 (C), 133.79 (C), 131.48 (2CH), 131.16 (C), 128.72 (2CH), 128.41 (2CH), 128.11 (CH), 127.60 (CH), 127.47 (2CH), 126.71 (2CH), 119.72 (C), 115.16 (2CH), 67.41 (CH_2), 55.49 (CH_2), 53.72 ($2CH_2$), 51.89 (CH_2), 28.59 (CH_2), 25.40 (CH_2), 23.67 (CH_2), 23.39 ($2CH_2$) ppm; HRMS (ESI): calcd. for $C_{30}H_{34}N_4O$ $[M+H]^+$, 467.2766; found: 467.2802.

4.1.4.14. 1-(5-(4-(1-Benzyl-4-phenyl-1H-1,2,3-triazol-5-yl)phenoxy) pentyl)piperidine (8n). Yield: 72% (80 mg); ^{1}H NMR (400 MHz, $CDCl_3$) δ 7.57 (dd, J = 8.0, 1.4, 2H), 7.28–7.24 (m, 6H), 7.07–7.03 (m, 4H), 6.90 (d, J = 8.7, 2H), 5.39 (s, 2H), 4.00 (t, 2H), 2.78 (s, 4H), 2.69 (t, 2H), 2.28 (t, 2H), 1.85–1.79 (m, 6H), 1.58–1.52 (m, 4H); ^{13}C NMR (126 MHz, $CDCl_3$) δ = 160.01 (C), 144.42 (C), 135.58 (C), 133.82 (C), 131.42 (2CH), 131.13 (C), 128.71 (2CH), 128.41 (2CH), 128.10 (CH), 127.59 (2CH), 126.66 (2CH), 119.49 (C), 115.11 (2CH), 67.71 (CH_2), 58.57 (CH_2), 54.11 ($2CH_2$), 51.87 (CH_2), 28.91 (CH_2), 25.39 (CH_2), 24.53 ($2CH_2$), 23.96 (CH_2), 23.49 (CH_2) ppm; HRMS (ESI): calcd. for $C_{31}H_{36}N_4O$ $[M+H]^+$, 481.2923; found: 481.2963.

4.1.4.15. 4,5-Diphenyl-1-(4-(3-(pyrrolidin-1-yl)propoxy)benzyl)-1H-1,2,3-triazole (8o). Yield: 70% (76 mg); ^{1}H NMR (400 MHz, $CDCl_3$) δ 7.54 (dd, J = 7.7, 1.9, 2H), 7.50–7.45 (m, 2H), 7.25–7.24 (m, 4H), 7.16 (d, J = 6.8, 2H), 6.97 (d, J = 8.5, 2H), 6.74 (d, J = 8.6, 2H), 5.33 (s, 2H), 4.04 (t, 2H), 3.84 (s, 2H), 3.27 (s, 2H), 2.83 (s, 2H), 2.42 (s, 2H), 2.25 (s, 2H), 2.09 (s, 2H); ^{13}C NMR (101 MHz, $CDCl_3$) δ 158.10 (C), 144.54 (C), 133.75 (C), 130.93 (C), 130.16 (2CH), 129.75 (CH), 129.23 (2CH), 129.21 (2CH), 128.45 (2CH), 128.21 (C), 127.96 (C), 127.72 (CH), 126.71 (2CH), 114.54 (2CH), 64.78 (CH_2), 53.92 ($2CH_2$), 53.27 (CH_2), 51.48 (CH_2), 25.76 (CH_2), 23.45 ($2CH_2$) ppm; HRMS (ESI): calcd. for $C_{28}H_{30}N_4O$ $[M+H]^+$, 439.2453; found: 439.2491.

4.1.4.16. 1-(4-Methoxybenzyl)-4-(4-methoxyphenyl)-5-(4-(3-(pyrrolidin-1-yl)propoxy)phenyl)-1H-1,2,3-triazole (8p). Yield: 75% (80 mg); ^{1}H NMR (400 MHz, $CDCl_3$) δ 7.48 (d, J = 8.9, 1H), 7.08–6.89 (m, 3H), 6.83–6.74 (m, 2H), 5.31 (s, 1H), 4.09 (t, 1H), 3.77 (s, 3H), 2.78–2.70 (m, 1H), 2.65 (s, 2H), 2.13–2.06 (m, 1H), 1.87–1.81 (m, 2H); ^{13}C NMR (126 MHz, $CDCl_3$) δ = 159.83 (C), 159.37 (C), 159.08 (C), 144.33 (C), 132.81 (C), 131.50 (2CH), 129.00 (2CH), 127.93 (2CH), 127.69 (C), 123.79 (C), 119.79 (C), 115.10 (2CH), 114.00 (2CH), 113.84 (2CH), 66.34 (CH_2), 55.29 (OCH_3), 55.20 (OCH_3), 54.19 (2CH), 53.10 (CH_2), 51.41 (CH_2), 28.44 (CH_2), 23.45 (2CH) ppm; HRMS (ESI): calcd. for $C_{30}H_{34}N_4O_3$ $[M+H]^+$, 499.2664; found: 499.2692.

4.1.4.17. N,N-diethyl-3-(4-(1-(4-methoxybenzyl)-4-(4-methoxyphenyl)-1H-1,2,3-triazol-5-yl)phenoxy)-propan-1-amine (8q). Yield: 73% (79 mg); ^{1}H NMR (400 MHz, $CDCl_3$) δ 7.48 (d, J = 8.8 Hz, 2H), 7.04 (d, J = 8.6 Hz, 2H), 6.96 (dd, J = 18.3, 8.6 Hz, 4H), 6.78 (dd, J = 8.5, 6.2 Hz, 4H), 5.31 (s, 2H), 4.07 (t, J = 6.3 Hz, 2H), 3.77 (s, 6H), 2.67–2.62 (m, 2H), 2.57 (dd, J = 14.3, 7.1 Hz, 4H), 1.46 (dt, J = 15.4, 7.8 Hz, 2H), 1.05 (t, J = 7.1 Hz, 6H); ^{13}C NMR (101 MHz, $CDCl_3$) δ 161.40 (C), 160.85 (C), 160.55 (C), 145.73 (C), 134.25 (C), 132.90 (2CH), 130.40 (2CH), 129.34 (2CH), 129.14 (C), 125.30 (C), 121.19 (C), 116.57 (2CH), 115.45 (2CH), 115.28 (2CH), 67.88 (OCH_2), 56.67(OCH_3), 56.59 (OCH_3), 52.82 (CH_2), 50.79 (CH_2), 48.47 ($2CH_2$), 28.37 (CH_2), 13.07 ($2CH_3$) ppm; ESI-MS (m/z): 501.0 $[M+H]^+$.

4.2. Experimental protocols

4.2.1. Cell lines, cell culture, growth conditions and reagents

A panel of human cancer cell lines namely MCF-7(Breast), HCT-116(Colon) [27–29], MDA-MB-231(Breast), FR-2 (normal breast epithelial) were purchased from ATCC for screening of (**6a-6d**) and (**8a-8s**) anticancer test molecules. The cell lines were grown in T75 tissue culture flasks in complete growth medium (RPMI-1640 and DMEM) added with 10% FBS, 100 μg/mL streptomycin as well as 100 units/mL penicillin in humidified carbon dioxide incubator (New Brunswick, Galaxy 170R, Eppendorf) at 37 °C, 5% CO_2 with 95% relative humidity. DAPI (4′, 6-diamidino-2-phenylindole), Rhodamine-123, DCFDA (2′, 7′-dichlorofluorescein diacetate) were procured from Sigma-Aldrich (St. Louis, MO, USA). Sulforhodamine B dye purchased from Hi Media. Monolayer cultures of the above cell lines were trypsinised using 0.25% trypsin/EDTA (1 mM) solution. After the cells got detached, the activity of trypsin/EDTA solution was stoppedusing complete growth medium and centrifuged at 1000 rpm for 5 min. Cells were again dispersed in complete growth medium in tissue culture flasks and incubated in CO_2 incubator. When cells attained approx. 50–60% confluency, they were treated with target compounds dissolved in DMSO and the untreated control cultures with (DMSO, < 0.2%).

4.2.2. Cytotoxicity activity against different cancer cell lines

The in vitro cytotoxicity activity of target compounds (**6a-6d**) and (**8a-8p**) were carried out using SRB (Sulforhodamine B) assay method reported by Skehan et al. [30] For preliminary screening, optimum inoculum densities per well of MCF-7 (7000), MDA-MB-231 (10,000) and HCT-116 (7000) cell lines were seeded in 96-well flat bottom plates (NUNC). Tamoxifen citrate used as standard drug for reference. Briefly, 100 μL/well of cell suspensions were seeded in 96-well tissue culture plates and incubated for 24 h. When cells attained 50–60% confluency, then different concentrations of anticancer test compounds were incubated and kept for another 48 h. Next, after the completion of 48 h incubation, the cells were settled using 50% ice cold trichloroacetic acid (TCA) and kept at 4 °C for 1 h and the plates were washed thrice in aqueous medium and air dried. Once the plates dried, 100 μL/well SRB dye added and kept for half an hour at room temperature. Soon after, the plates were again washed thrice using 1% glacial acetic acid to eliminate excess unbound SRB and the plates were further air dried. When the plates were completely dried, the bound SRB was solubilized by adding 100μL/well 10 mM TRIS (tris(hydroxymethyl) aminomethane) buffer of pH 10.5 and plates were kept on orbital shaker for 5 min. Lastly, absorbance was recorded at 540 nm in

microplate reader (Tecan Infinite M Nano). IC_{50} was determined by Graph Pad Prism 6.0 (Graph Pad Software Inc, San Diego, CA, USA) software. Percent cell viability and percent inhibition was calculated using the following formula and were tested at least in triplicates [31].

% Growth inhibition = 100 - [Absorbance of treated cells/Absorbance of control cells x 100]

4.2.3. Treatment profile and dose selection

On the basis of the data obtained from the screening profile of different molecules, **8f** molecule possesses good anticancer activity against MCF-7 cell line bearing IC_{50} value of 3.5 μM. Therefore, in current study we have chosen 3.5 μM as an impressive dose of the anticancer test molecule **8f** for 48 h in addition to negative control (untreated) as well as 9.5 μM of standard moiety, tamoxifen citrate in 6-well tissue culture plates. By taking the above mentioned doses, further mechanistic studies were performed against MCF-7 cell line for 48 h time period.

4.2.4. Morphological examination of compound 8f under bright field microscopy

Morphological examination through bright field microscopy is the simplest technique to identify the surface morphological changes of cancer cells after the treatment with anticancer test molecules by comparing with untreated cells. In this experiment, MCF-7 cells were treated with IC_{50} 3.5 μM of **8f** for 48 h in addition to untreated control as well as 9.5 μM of standard moiety, tamoxifen in 6-well tissue culture plates. After the treatment, compound containing exhausted media was discarded and cells were washed with ice cold PBS. Further, all the wells were incubated with incomplete growth medium and cells were imaged under bright field inverted microscope (Olympus 10X) (Fig. 3) [32].

4.2.5. Apoptosis assay through DAPI staining

In order to examine apoptotic cell death qualitatively, morphological variations in chromatin structure were detected using DAPI staining. Precisely, MCF-7 cells at a density of 1×10^5 were seeded in a 6-well tissue culture plates and kept for 24 h to attain confluency about 50–60% and treatment was given to the plate with above mentioned concentration of compound **8f** and tamoxifen used as standard positive control drug kept for another 48 h incubation. Later, cells were washed with ice cold PBS to remove dead cell moieties. Again cells were fixed using 70% ethanol for 1 h at room temperature and washed with cold PBS. Finally, the cells were stained with 1 μg/mL DAPI in dark for 5 min, washed with ice cold PBS and final volume of PBS added to each well and plate was observed under an inverted fluorescence microscope (Olympus, 1 × 70) [33].

4.2.6. Reactive oxygen species (ROS) generation assay

Dye 2′,7′-dichlorofluorescein diacetate (DCFH-DA) was used to measure intracellular ROS production. DCFH gets transformed into highly fluorescent 2′, 7′-dichlorofluorescein (DCF) in the presence of an oxidant. In this study, 1×10^5 MCF-7 cells were incubated for 24 h in a 6-well plates and 3.5 μM concentration of molecule **8f** and kept for further 48 h incubation. 0.05% H_2O_2 was used as standard positive control and added 1 h before conclusion of the experiment. The cells were washed with ice cold PBS and 10 μM DCFH-DA added to all the wells for 30 min in dark. Plate was further washed with cold PBS and final volume of incomplete media added to each well and finally observed under an inverted fluorescence microscope (Olympus, 1 × 70) [34].

4.2.7. Measurement of loss of mitochondrial membrane potential ($\Delta\Psi m$)

Mitochondrial perturbation occurs due to loss of membrane potential was studied using dye rhodamine-123 by fluorescence microscope qualitatively. Human breast cancer (MCF-7) cells (1×10^5/mL/well) were seeded in a 6-well tissue culture plates and treated with 3.5 μM concentration of molecule **8f** and tamoxifen used as standard positive control drug and incubated for 48 h. After treatment, cells were washed with ice cold PBS, later final concentration of 0.2 μM rhodamine incubated to all the wells and finally kept for 20–30 min in dark inside the incubator. Further, washed with cold PBS and final volume of incomplete media was added to all the wells and analyzed under fluorescence microscope (Olympus, 1 × 70) [35].

4.2.8. Statistical analysis

The results are interpreted as mean ± of SD belonging to three independent tests. Standard deviations were calculated using Graphpad prism 6.0 (Graph Pad Software Inc., San Diego, CA, USA) and Microsoft excel.

4.2.9. Molecular docking studies

The crystal structure of human ER-α (PDB ID: 3ERT) [31–36] [31] was retrieved from the protein data bank and was subjected to protein preparation steps under default settings in Schrodinger software. The ligands were drawn in ChemDraw. The docking protocol was validated by re-docking the co-crystallized ligand and comparing its interaction pattern. All steps of docking were as per default settings of Glide module of Schrodinger software.

Declaration of competing interest

The authors declare that they have no known competing financial interests or personal relationships that could have appeared to influence the work reported in this paper.

Acknowledgement

D.D., D.S. thank to CSIR-New Delhi, ICMR, and C.B., M.D. thank UGC, India for supporting research fellowship. This research work was financially supported by DST-EMR/2016/002304 and DST-EEQ/2016/000102.

References

[1] E. Vitaku, D.T. Smith, J.T. Njardarson, Analysis of the structural diversity, substitution patterns, and frequency of nitrogen heterocycles among U.S. FDA approved pharmaceuticals, J. Med. Chem. 57 (2014) 10257–10274.
[2] E.C. Franklin, Heterocyclic nitrogen compounds. I. Pentacyclic compounds, Chem. Rev. 16 (1935) 305–361.
[3] D. Dheer, V. Singh, R. Shankar, Medicinal attributes of 1,2,3-triazoles: current developments, Bioorg. Chem. 71 (2017) 30–54.
[4] J.A. Stefely, R. Palchaudhuri, P.A. Miller, R.J. Peterson, G.C. Moraski, P.J. Hergenrother, M.J. Miller, N-((1-Benzyl-1H-1,2,3-triazol-4-yl)methyl)arylamide as a new scaffold that provides rapid access to antimicrotubule agents: synthesis and evaluation of antiproliferative activity against select cancer cell lines, J. Med. Chem. 53 (2010) 3389–3395.
[5] N. Ashwini, M. Garg, C.D. Mohan, J.E. Fuchs, S. Rangappa, S. Anusha, T.R. Swaroop, K.S. Rakesh, D. Kanojia, V. Madan, A. Bender, H.P. Koeffler, Basappa, K.S. Rangappa, Synthesis of 1,2-benzisoxazole tethered 1,2,3-triazoles that exhibit anticancer activity in acute myeloid leukemia cell lines by inhibiting histone deacetylases, and inducing p21 and tubulin acetylation, Bioorg. Med. Chem. 23 (2015) 6157–6165.
[6] R. Majeed, P.L. Sangwan, P.K. Chinthakindi, I. Khan, N.A. Dangroo, N. Thota, A. Hamid, P.R. Sharma, A.K. Saxena, S. Koul, Synthesis of 3-O-propargylated betulinic acid and its 1,2,3-triazoles as potential apoptotic agents, Eur. J. Med. Chem. 63 (2013) 782–792.
[7] R.N. Khaybullin, M. Zhang, J. Fu, X. Liang, T. Li, A.R. Katritzky, P. Okunieff, X. Qi, Design and synthesis of isosteviol triazole conjugates for cancer therapy, Molecules 19 (2014) 18676–18689.
[8] J.L.C. Sousa, C.S.R. Freire, A.J.D. Silvestre, A.M.S. Silva, Recent developments in

the functionalization of betulinic acid and its natural analogues: a route to new bioactive compounds, Molecules 24 (2019) 355.
[9] B. Aneja, M. Azam, S. Alam, A. Perwez, R. Maguire, U. Yadava, K. Kavanagh, C.G. Daniliuc, M.M.A. Rizvi, Q.M.R. Haq, M. Abid, Natural product-based 1,2,3-triazole/sulfonate analogues as potential chemotherapeutic agents for bacterial infections, ACS Omega 3 (2018) 6912–6930.
[10] M. Smollich, M. Gotte, J. Fischgrabe, I. Radke, L. Kiesel, P. Wulfing, Differential effects of aromatase inhibitors and antiestrogens on estrogen receptor expression in breast cancer cells, Anticancer Res. 29 (2009) 2167–2171.
[11] C. Williams, A. DiLeo, Y. Niv, J. Gustafsson, Estrogen receptor beta as target for colorectal cancer prevention, Canc. Lett. 372 (2016) 48–56.
[12] R. Kennelly, D.O. Kavanagh, A.M. Hogan, D.C. Winter, Oestrogen and the colon: potential mechanisms for cancer prevention, Lancet Oncol. 9 (2008) 385–391.
[13] L.J. Lerner, V.C. Jordan, Development of antiestrogens and their use in breast cancer: eighth Cain memorial award lecture, Canc. Res. 50 (1990) 4177–4189.
[14] A.L. Taylor, L.L. Adams-Campbell, J. Wright, Risk/benefit assessment of tamoxifen to prevent breast cancerstill a work in progress? J. Natl. Cancer Inst. (Bethesda) 91 (1999) 1792–1793.
[15] B.E. Fink, D.S. Mortensen, S.R. Stauffer, Z.D. Aron, J.A. Katzenellenbogen, Novel structural templates for estrogen-receptor ligands and prospects for combinatorial synthesis of estrogens, Chem. Biol. 6 (1999) 205–219.
[16] S.R. Stauffer, C.J. Coletta, R. Tedesco, G. Nishiguchi, K. Carlson, J. Sun, B.S. Katzenellenbogen, J.A. Katzenellenbogen, Pyrazole ligands: structure-affinity/activity relationships and estrogen receptor-alpha-selective agonists, J. Med. Chem. 43 (2000) 4934–4947.
[17] S.R. Stauffer, Y.R. Huang, Z.D. Aron, C.J. Coletta, J. Sun, B.S. Katzenellenbogen, J.A. Katzenellenbogen, Triarylpyrazoles with basic side chains: development of pyrazole-based estrogen receptor antagonists, Bioorg. Med. Chem. 9 (2001) 151–161.
[18] U.S. Singh, R. Shankar, G.P. Yadav, G. Kharkwal, A. Dwivedi, G. Keshri, M.M. Singh, P.R. Moulik, K. Hajela, Synthesis and structure guided evaluation of estrogen agonist and antagonist activities of some new tetrazolyl indole derivatives, Eur. J. Med. Chem. 43 (2008) 2149–2158.
[19] R. Shankar, B. Chakravarti, U.S. Singh, M.I. Ansari, S. Deshpande, S.K.D. Dwivedi, H.K. Bid, R. Konwar, G. Kharkwal, V. Chandra, A. Dwivedi, K. Hajela, Synthesis and biological evaluation of 3,4,6-triaryl-2-pyranones as a potential new class of anti-breast cancer agents, Bioorg. Med. Chem. 17 (2009) 3847–3856.
[20] R. Shankar, R. Rawal, U.S. Singh, P. Chaudhary, R. Konwar, K. Hajela, Design, synthesis and biological evaluation of hydrazone derivatives as anti-proliferative agents, Med. Chem. Res. 26 (2017) 1459–1468.
[21] J.A. Pollock, N. Sharma, S.K. Ippagunta, V. Redecke, H. Hacker, J.A. Katzenellenbogen, Triaryl pyrazole toll-like receptor signaling inhibitors: structure-activity relationships governing pan- and selective signaling inhibitors, ChemMedChem 13 (2018) 2208–2216.
[22] D. Dheer, R. Rawal, V. Singh, P.L. Sangwan, P. Das, R. Shankar, β-CD/CuI catalyzed regioselective synthesis of iodo substituted 1,2,3-triazoles, imidazo[1,2-a]-pyridines and benzoimidazo[2,1-b]thiazoles in water and their functionalization, Tetrahedron 73 (2017) 4295–4306.
[23] N. Miyaura, A. Suzuki, Palladium-catalyzed cross-coupling reactions of organoboron compounds, Chem. Rev. 95 (1995) 2457–2483.
[24] S. Xu, H.-H. Chen, J.-J. Dai, H.-J. Xu, Copper-promoted reductive coupling of aryl iodides with 1,1,1-trifluoro-2-iodoethane, Org. Lett. 16 (2014) 2306–2309.
[25] L. Ackermann, R. Vicente, R. Born, Palladium-catalyzed direct arylations of 1,2,3-triazoles with aryl chlorides using conventional heating, Adv. Synth. Catal. 350 (2008) 741–748.
[26] O.A. Peña-Morán, M.L. Villarreal, L. Álvarez-Berber, A. Meneses-Acosta, V. Rodríguez-López, Cytotoxicity, post-treatment recovery, and selectivity analysis of naturally occurring podophyllotoxins from Bursera fagaroides var. fagaroides on breast cancer cell lines, Molecules 21 (2016) 1013.
[27] R.T. Chlebowski, J. Wactawski-Wende, C. Ritenbaugh, F.A. Hubbell, J. Ascensao, R.J. Rodabough, C.A. Rosenberg, V.M. Taylor, R. Harris, C. Chen, L.L. Adams-Campbell, E. White, Estrogen plus progestin and colorectal cancer in postmenopausal women, N. Engl. J. Med. 350 (2004) 991–1004.
[28] A. Hendifar, D. Yang, F. Lenz, G. Lurje, A. Pohl, C. Lenz, Y. Ning, W. Zhang, H.-J. Lenz, Gender disparities in metastatic colorectal cancer survival, Clin. Canc. Res. 15 (2009) 6391–6397.
[29] M.D. Long, C.F. Martin, J.A. Galanko, R.S. Sandler, Hormone replacement therapy, oral contraceptive use, and distal large bowel cancer: a population-based case-control study, Am. J. Gastroenterol. 105 (2010) 1843–1850.
[30] P. Skehan, R. Storeng, D. Scudiero, A. Monks, J. McMahon, D. Vistica, J.T. Warren, H. Bokesch, S. Kenney, M.R. Boyd, New colorimetric cytotoxicity assay for anticancer-drug screening, J. Natl. Cancer Inst. 82 (1990) 1107–1112.
[31] V. Sharma, A. Qayum, S. Kaul, A. Singh, K.K. Kapoor, D. Mukherjee, S.K. Singh, M.K. Dhar, Carbohydrate modifications of neoandrographolide for improved reactive oxygen species-mediated apoptosis through mitochondrial pathway in colon cancer, ACS Omega 4 (2019) 20435–20442.
[32] M.I. Ansari, M.K. Hussain, A. Arun, B. Chakravarti, R. Konwar, K. Hajela, Synthesis of targeted dibenzo[b,f]thiepines and dibenzo[b,f]oxepines as potential lead molecules with promising anti-breast cancer activity, Eur. J. Med. Chem. 99 (2015) 113–124.
[33] Y.H. Kang, E. Lee, M.K. Choi, J.L. Ku, S.H. Kim, Y.G. Park, S.J. Lim, Role of reactive oxygen species in the induction of apoptosis by alpha-tocopheryl succinate, Int. J. Canc. 112 (2004) 385–392.
[34] S.K. Kim, G.J. Im, Y.S. An, S.H. Lee, H.H. Jung, S.Y. Park, The effects of the antioxidant α-tocopherol succinate on cisplatin-induced ototoxicity in HEI-OC1 auditory cells, Int. J. Pediatr. Otorhinolaryngol. 86 (2016) 9–14.
[35] A. Kumar, B. Singh, G. Mahajan, P.R. Sharma, S.B. Bharate, M.J. Mintoo, D.M. Mondhe, A novel colchicine-based microtubule inhibitor exhibits potent antitumor activity by inducing mitochondrial mediated apoptosis in MIA PaCa-2 pancreatic cancer cells, Tumour Biol 37 (2016) 13121–13136.
[36] S. Patel, L. Vuillard, A. Cleasby, C.W. Murray, J. Yon, Apo and inhibitor complex structures of BACE (beta-secretase), J. Mol. Biol. 343 (2004) 407–416.